

# Delayed Stochastic Algorithms for Distributed Weakly Convex Optimization

Wenzhi Gao\* and Qi Deng†

Shanghai University of Finance and Economics

January 31, 2023

## Abstract

This paper studies delayed stochastic algorithms for weakly convex optimization in a distributed network with workers connected to a master node. More specifically, we consider a structured stochastic weakly convex objective function which is the composition of a convex function and a smooth nonconvex function. Recently, Xu et al. 2022 showed that an inertial stochastic subgradient method converges at a rate of  $\mathcal{O}(\tau/\sqrt{K})$ , which suffers a significant penalty from the maximum information delay  $\tau$ . To alleviate this issue, we propose a new delayed stochastic prox-linear (DSPL) method in which the master performs the proximal update of the parameters and the workers only need to linearly approximate the inner smooth function. Somewhat surprisingly, we show that the delays only affect the high order term in the complexity rate and hence, are negligible after a certain number of DSPL iterations. Moreover, to further improve the empirical performance, we propose a delayed extrapolated prox-linear (DSEPL) method which employs Polyak-type momentum to speed up the algorithm convergence. Building on the tools for analyzing DSPL, we also develop an improved analysis of the delayed stochastic subgradient method (DSGD). In particular, for general weakly convex problems, we show that convergence of DSGD only depends on the expected delay.

## 1 Introduction

We consider the following stochastic optimization problem

$$\min_{x \in \mathbb{R}^n} \psi(x) := \mathbb{E}_{\xi \sim \Xi} [f(x, \xi)] + \omega(x), \quad (1)$$

where  $f(x, \xi)$  is a nonconvex continuous function over  $x$  and  $\xi$  is a random variable sampled from some distribution  $\Xi$ ;  $\omega(x)$  is lower-semicontinuous and proximal-friendly. We assume that both  $f(x, \xi)$  and  $\omega(x)$  belong to a general class of nonsmooth nonconvex functions that exhibit weak convexity. Here, we say that a function  $g(x)$  is  $\kappa$ -weakly convex if the sum  $g(x) + \frac{\kappa}{2}\|x\|^2$  is convex for some  $\kappa \geq 0$ . Weakly convex optimization has attracted growing interest in machine learning in recent years. We are particularly interested in a general type of weakly convex problems with the following composition structure [13]

$$f(x, \xi) = h(c(x, \xi)), \quad (2)$$

where  $h$  is a convex Lipschitz function and  $c(x, \xi)$  is smooth. Optimization in the above composition form is pervasive in applications arising from machine learning and data science, including robust phase retrieval [15], blind deconvolution [8], robust PCA and matrix completion [5], among others.

---

\*Email: gwz@163.shufe.edu.cn

†Email: qideng@sufe.edu.cn

In a broader context, stochastic (sub)gradient method and its proximal variants [32, 30, 34] (all referred as SGD in our paper, for brevity) are arguably the most popular approaches for solving problem (1). Typically, SGD iteratively solves  $x^{k+1} = \arg \min_x \langle f'(x^k, \xi^k), x - x^k \rangle + \omega(x) + \frac{\gamma_k}{2} \|x - x^k\|^2$ , where  $\xi^k$  is a random sample and  $f'(x^k, \xi^k)$  denotes a subgradient of  $f(x^k, \xi^k)$ . However, despite its wide popularity in machine learning, the sequential and synchronous nature of SGD is not suitable for modern applications that require parallel processing in multi-cores or over multiple machines for further acceleration.

To further improve the efficiency of SGD in parallel and distributed environment, recent work considers a more practical asynchronous setting such that the parameter update allows out-of-date gradient information. See Agarwal and Duchi [1], Sra et al. [35], Zheng et al. [43], Recht et al. [31], Lian et al. [22]. In the asynchronous setting, it is crucial to know how the stale updates based on delayed information affects algorithm convergence. For smooth convex optimization, Agarwal and Duchi [1] shows that delayed stochastic gradient method obtains a rate of  $\mathcal{O}(\frac{\sigma}{\sqrt{K}} + \frac{\tau^2}{\sigma^2 K})$ , where  $\tau$  is an upper-bound of the possible delay. DSGD with adaptive stepsize has also been studied by [27, 35, 43] to achieve better empirical performance. [16] improves the convergence rate to  $\mathcal{O}(\frac{\sigma}{\sqrt{K}} + \frac{\tau}{K})$  and the latest work [2, 36] further improves the rate to  $\mathcal{O}(\frac{\sigma}{\sqrt{K}} + \frac{\tau}{K})$ . For general smooth (nonconvex) problems, [36] shows that DSGD converges to stationarity at a rate of  $\mathcal{O}(\frac{\sigma}{\sqrt{K}} + \frac{\tau}{K})$ . In a follow-up study [7], the authors propose a more robust DSGD whose rate depends on the average rather than the maximum delay. Based on novel delay-adaptive stepsizes and virtual iterate-based analysis, Mishchenko et al. [28] establishes new convergence rates of DSGD that are dependent on the number of workers rather than the delay on the gradient.

Despite much progress in distributed smooth optimization, it remains unclear how to develop efficient asynchronous algorithms for nonsmooth, and even nonconvex problems. For general convex problems, the pioneering work [29] has shown that the asynchronous incremental subgradient method obtains an  $\mathcal{O}(\sqrt{\frac{\tau}{K}})$  convergence rate. The mentioned work [28] shows that DSGD achieves a delay-independent rate of  $\mathcal{O}(\sqrt{\frac{m}{K}})$ , where  $m$  is the number of workers. However, it is still unknown whether their key technique by telescoping the virtual iterates can be extended to composite and nonconvex optimization.

For distributed weakly convex optimization, Xu et al. [38] shows that DSEGD (Delayed Stochastic Extrapolated Subgradient Method), the inertial version of DSGD, exhibits a convergence rate of  $\mathcal{O}(\frac{1+\tau}{\sqrt{K}} + \frac{\tau}{K})$ , which has an undesired dependence on the maximum delay  $\tau$ . This issue is further exacerbated in real heterogeneous environments where the maximum delay is determined by the slowest machine. *It remains unclear whether such delay dependence in DSGD is still improvable or not.* Nevertheless, even if the rate is improvable in terms of  $\tau$ , there yet remains a fundamental challenge in the analysis of DSGD, as delay has a major impact on the leading term  $\mathcal{O}(\frac{1}{\sqrt{K}})$  of the convergence rate. This is in contrast to smooth distributed optimization where delay only affects a higher order term  $\mathcal{O}(\frac{1}{K})$  and hence is negligible in the long run. Such performance gap highlights a substantial limitation of DSGD when nonsmoothness is present. Hence, it is natural to ask the following question:

*For nonsmooth nonconvex optimization, can we design an efficient stochastic algorithm which has a negligible penalty caused by delays?*

To address this question, we intend to further exploit the structure information of (2). To this end, we consider the **Stochastic Prox-Linear** (SPL) algorithm [14, 8]. Different from subgradient-based methods, SPL partially linearizes the inner function  $c(\cdot, \xi)$  while retaining the outer function  $h(\cdot)$ . Then it solves the following proximal problem iteratively:

$$x^{k+1} = \arg \min_x \{h(c(x^k, \xi^k) + \langle \nabla c(x^k, \xi^k), x - x^k \rangle) + \omega(x) + \frac{\gamma_k}{2} \|x - x^k\|^2\}. \quad (3)$$

In the seminal work by Davis and Drusvyatskiy [8], the authors show that while SPL obtains the same  $\mathcal{O}(\frac{1}{\sqrt{K}})$  rate of SGD, SPL exhibits much more robust empirical performance to the stepsize selection. Recently, Deng

and Gao [12] shows that minibatch SPL can be linearly accelerated over the batchsize even though the problem is nonsmooth, while such a property is not known for SGD.

## 1.1 Contributions

In this work, we apply SPL in a distributed network in which the workers compute the smooth function value  $c(\cdot, \xi)$  and its gradient while the master performs an update by solving a proximal map associated with  $h(\cdot)$ . However, instead of receiving the current information, the master may get outdated values  $c(x^{k-\tau_k}, \xi^{k-\tau_k})$  and  $\nabla c(x^{k-\tau_k}, \xi^{k-\tau_k})$ , where  $\tau_k$  is a random delay at round  $k$ . Our main contribution is to show that the delayed stochastic prox-linear method (DSPL) obtains an  $\mathcal{O}(\frac{1}{\sqrt{K}} + \frac{\bar{\tau} + \tau_{\sigma^2}}{K})$  rate of convergence, where  $\bar{\tau}$  is the expected delay and  $\tau_{\sigma^2}$  is delay's second moment. Hence, DSPL consistently outperforms DSGD in terms of the dependence on  $\tau$ , for any meaningful value of  $K$  (i.e.  $K \gg \tau^2$ , otherwise, the bound is trivial). More interestingly and somewhat surprisingly, if  $\max\{\bar{\tau}, \tau_{\sigma^2}\} = o(K^{1/2})$ , our rate reduces to  $\mathcal{O}(\frac{1}{\sqrt{K}})$ , which implies that the delay is negligible when  $K$  is sufficiently large. In addition, due to the attractive empirical advantage of the momentum technique [37], we provide a new delayed extrapolated prox-linear algorithm (DSEPL) using Polyak-type momentum. We show that the momentum-based algorithm remains tolerant of large delays. To the best of our knowledge, our complexity results are the first ones in the distributed stochastic weakly convex setting where the effect of delay is proven negligible.

Apart from contributing new distributed algorithms, we also develop improved convergence analysis of DSGD by alleviating the dependence on information delay. Using a similar analysis developed for DSPL, we show that when  $f(x)$  is smooth, the proximal DSGD also achieves a rate of  $\mathcal{O}(\frac{1}{\sqrt{K}} + \frac{\bar{\tau} + \tau_{\sigma^2}}{K})$ . When  $f$  is general weakly-convex, we show that proximal DSGD achieves a rate of  $\mathcal{O}(\frac{\bar{\tau}}{\sqrt{K}})$ . Both convergence rates significantly improve the earlier results [38] which have a dependence on the maximum delay. A summary of our contribution and a more detailed comparison are provided in Table 1.

Objective	Methods	Best [38]	Ours
$f + \omega$ Lip.	DSGD & DSEGD	Both $\mathcal{O}(\frac{\bar{\tau}}{\sqrt{K}})$	$\mathcal{O}(\frac{\bar{\tau}}{\sqrt{K}})$ & —
$f$ smooth + $\omega$ Lip.	DSGD & DSEGD	Both $\mathcal{O}(\frac{1}{\sqrt{K}} + \frac{\tau^2}{K})$	$\mathcal{O}(\frac{1}{\sqrt{K}} + \frac{\bar{\tau} + \tau_{\sigma^2}}{K})$ & $\mathcal{O}(\frac{1}{\sqrt{K}} + \frac{\tau^2}{K})$
$f \circ g + \omega$ , $f, \omega$ Lip, $g$ smooth	DSPL & DSEPL	—	$\mathcal{O}(\frac{1}{\sqrt{K}} + \frac{\bar{\tau} + \tau_{\sigma^2}}{K})$ & $\mathcal{O}(\frac{1}{\sqrt{K}} + \frac{\tau^2}{K})$

Table 1: Convergence rates on stochastic weakly convex optimization.  $\tau$ : maximum delay,  $\bar{\tau}$ : expected delay and  $\tau_{\sigma^2}$ : the second moment of delay. Convergence rates are measured by  $\|\nabla \psi_{1/\rho}\|^2$ . E: extrapolation.

**Structure of the paper** Section 2 introduces the notations and problem setup. Section 3 develops the delayed stochastic prox-linear method (DSPL). Section 4 proposes a momentum extension DSEPL and analyzes its convergence. Section 5 develops an improved analysis of the delayed stochastic (proximal)subgradient method. Section 6 conducts experiments to compare our proposed methods with SGD. Finally, we draw conclusions in Section 7. We leave all the proofs and additional experiments in the appendix.

## 2 Preliminaries

**Notations** We use  $\|\cdot\|$  and  $\langle \cdot, \cdot \rangle$  to denote the Euclidean norm and inner product. The sub-differential of a function  $f$  is defined by  $\partial f(x) := \{v : f(y) \geq f(x) + \langle v, y - x \rangle + o(\|x - y\|), y \rightarrow x\}$  and  $f'(x) \in \partial f(x)$  denotes a subgradient. If  $0 \in \partial f(x)$ , then  $x$  is called a stationary point of  $f$ . The domain of  $f$  is defined by  $\text{dom } f := \{x : f(x) < \infty\}$ . At iteration  $k$ , we use  $\mathbb{E}_k[\cdot] = \mathbb{E}_{\xi_k}[\cdot | \sigma_k]$  to abbreviate the  $\sigma$ -algebra generating  $\{\xi_j, j \leq k\}$ .

Our main convergence analysis will adopt the Moreau-envelope function as the potential function, which was initially identified in the work [8]. Given parameter  $\rho > 0$ , the Moreau envelope and the associated proximal mapping of  $f$  are defined by

$$f_{1/\rho}(x) := \min_y \{f(y) + \frac{\rho}{2}\|x - y\|^2\} \quad \text{and} \quad \text{prox}_{f/\rho}(x) := \arg \min_y \{f(y) + \frac{\rho}{2}\|x - y\|^2\},$$

Suppose that  $f$  is  $\kappa$ -weakly convex for some  $\kappa < \rho$ . By the optimality condition and convexity of  $f(y) + \frac{\rho}{2}\|x - y\|^2$ ,  $0 \in \partial f(\text{prox}_{f/\rho}(x)) + \rho(\text{prox}_{f/\rho}(x) - x)$ . Moreover, the Moreau envelope can be interpreted as a smooth approximation of the original function. Specifically, it can be shown that  $f_{1/\rho}(x)$  is differentiable and its gradient is given by  $\nabla f_{1/\rho}(x) = \rho(x - \text{prox}_{f/\rho}(x))$  [8]. Combining the above two relations, we obtain  $\nabla f_{1/\rho}(x) \in \partial f(\text{prox}_{f/\rho}(x))$ . Therefore, the Moreau envelope can be used as a measure of approximate stationarity: if  $\|\nabla f_{1/\rho}(x)\| \leq \varepsilon$ , then  $x$  is in the proximity (i.e.  $\|x - \text{prox}_{f/\rho}(x)\| \leq \rho^{-1}\varepsilon$ ) of a near stationary point  $\text{prox}_{f/\rho}(x)$  (i.e.  $\text{dist}(\partial f(\text{prox}_{f/\rho}(x)), 0) \leq \varepsilon$ ).

## 2.1 Assumptions

Throughout the paper, we make the following assumptions. The first two assumptions are common in stochastic weakly convex optimization.

**A1:** (I.i.d. sample) We draw i.i.d. samples  $\{\xi^k\}$  from  $\Xi$ .

**A2:** (Lipschitz continuity)  $\omega(x)$  is  $L_\omega$ -Lipschitz continuous over its domain.

**A3:** (Weak convexity)  $\omega$  is  $\kappa$ -weakly convex.

**A4:** (Bounded moment) The distribution of the stochastic delays  $\{\tau_k\}$  has bounded the first and second moments.  
i.e.,  $\mathbb{E}[\tau_k] \leq \bar{\tau} < \infty, \mathbb{E}[\tau_k^2] \leq \tau_{\sigma^2} < \infty, \forall k$ .

*Remark 1.* **A4** is satisfied by common delay distributions, such as uniform [35], geometric and Poisson distribution [3].

## 3 Delayed Stochastic Prox-linear Method

In this section, we present a delayed stochastic prox-linear method (DSPL) for composite optimization problem with  $f(x, \xi) = h(c(x, \xi))$ , where  $h$  is convex nonsmooth and  $c$  is smooth and possibly nonconvex. For brevity, we denote  $f_z(x, \xi) = h(c(z, \xi) + \langle \nabla c(z, \xi), x - z \rangle)$ , a partial linearization of objective, and we use these two notations interchangeably for describing DSPL. As we will show later, this linearization scheme improves the accuracy when approximating the original objective, thus giving improving convergence results when there is delayed information.

We describe DSPL in Algorithm 1. DSPL can be deployed in a multi-agent network where all the workers are connected to a master server. We assume that the workers have access to random samples  $\xi$  and compute the function value  $c(x, \xi)$  and gradient  $\nabla c(x, \xi)$ . At the  $k$ -th iteration, the master node receives a delayed value  $c(x^{k-\tau_k}, \xi^{k-\tau_k})$  and gradient  $\nabla c(x^{k-\tau_k}, \xi^{k-\tau_k})$  of an earlier point  $x^{k-\tau_k}$ . Next, it performs a proximal update (4) to obtain the next iterate  $x^{k+1}$ . Throughout the rest of this paper, we assume that the proximal update is easy to compute. We also assume that only a single pair of  $c(x, \xi)$  and  $\nabla c(x, \xi)$  is obtained per iteration. In a minibatch setting, one can either invoke a fast solver [12] or run several iterations of (4) to pass through the minibatch.

To derive the convergence results of DSPL, we now formally state the assumptions on  $h$  and  $c$ .

**B1:**  $h(x)$  is convex and  $L_h$ -Lipschitz continuous;  $c(x, \xi)$  has  $C$ -Lipschitz continuous gradient and is  $L_c$  Lipschitz-continuous over  $\text{dom } \omega, \forall \xi \sim \Xi$ .

---

**Algorithm 1:** Delayed stochastic prox-linear

---

**Input:**  $x^1$ ;  
**for**  $k = 1, 2, \dots$  **do**  
    Let  $c(x^{k-\tau_k}, \xi^{k-\tau_k})$  and  $\nabla c(x^{k-\tau_k}, \xi^{k-\tau_k})$  be computed by a worker with delay  $\tau_k$ ;  
    In the master node update  

$$x^{k+1} = \arg \min_x \{f_{x^{k-\tau_k}}(x, \xi^{k-\tau_k}) + \omega(x) + \frac{\gamma_k}{2} \|x - x^k\|^2\} \quad (4)$$
  
**end**

---

*Remark 2.* On one hand, we note that generally Lipschitz continuity of  $c$  can be imposed by restricting domain of  $\omega$  to a bounded set. On the other hand, in the appendix we propose a more elegant solution using Bregman proximal iteration and relative Lipschitz condition to relax this assumption. Namely we replace Euclidean regularization  $\frac{1}{2}\|x - x_k\|^2$  in (3) by some divergence  $V_d(x, x^k)$  generated from some strongly convex function  $d$ .

Under the assumptions, the stochastic model  $f_z(x, \xi)$  can be shown to satisfy the following desirable properties

**Proposition 1** (Properties of  $f_z(x, \xi)$ ).

- P1:**  $f_z(x, \xi)$  is convex,  $\forall x, z \in \text{dom } \omega, \xi \sim \Xi$ .
- P2:**  $|f_z(x, \xi) - f(x, \xi)| \leq \frac{L_h C}{2} \|x - z\|^2, \forall x, z \in \text{dom } \omega, \xi \sim \Xi$ .
- P3:**  $f_z(x, \xi) - f_z(y, \xi) \leq L_h L_c \|y - x\|, \forall x, y, z \in \text{dom } \omega, \xi \sim \Xi$

From **Proposition 1**, we see  $f(x, \xi)$  is  $L_h C$ -weakly convex since the error between  $f(x, \xi)$  (or  $f(x)$ ) and a convex function is bounded by a quadratic function. For a unified analysis, we take  $L_f = L_h L_c, \lambda = L_h C$  and use these constants to present the results.

In this paper the clue of our analysis adopts variants of Moreau envelope  $\mathbb{E}_k[\psi_{1/\rho}(\hat{x}^k)]$  as the potential function and after measuring the decent of the potential function, we derive the convergence result by bounding the deviation caused by stochastic delays.

The following lemma characterizes a descent property of the potential function in DSPL.

**Lemma 1.** Under **A1** to **A3** as well as **B1**, if  $\rho \geq 2\lambda + \kappa, \gamma_k \geq \rho$ , then

$$\begin{aligned}
 \frac{\rho(\rho - 2\lambda - \kappa)}{2(\gamma_k - 2\lambda - \kappa)} \|\hat{x}^k - x^k\|^2 &\leq \psi_{1/\rho}(x^k) - \mathbb{E}_k[\psi_{1/\rho}(x^{k+1})] \\
 &\quad + \frac{2\rho L_f^2}{\gamma_k(\gamma_k - 2\lambda - \kappa)} + \frac{3\rho\lambda}{2(\gamma_k - 2\lambda - \kappa)} \mathbb{E}_k[\|x^{k+1} - x^{k-\tau_k}\|^2].
 \end{aligned}$$

*Remark 3.* **Lemma 1** shows that aside from the noise and delay-related terms, unless we are close to approximate stationarity characterized by  $\|\hat{x}^k - x^k\|^2$ , there is always a sufficient decrease in the potential function. Intuitively, as long as we take sufficiently large regularization  $\gamma$  and manage to bound the deviation from delays using **A4**, the convergence result is almost immediate.

Invoking **A4** we obtain the final convergence result.

**Theorem 1.** Under the same conditions as **Lemma 1**, taking  $\gamma = 2\lambda + \kappa + \sqrt{K}/\alpha > \rho$  for some  $\alpha > 0$  and letting  $k^*$  be an index chosen from  $\{1, \dots, K\}$  uniformly at random,

$$\mathbb{E}[\|\nabla \psi_{1/\rho}(x^{k^*})\|^2] \leq \frac{2\rho}{\rho - 2\lambda - \kappa} \left[ \frac{D}{\sqrt{K}\alpha} + \frac{2\rho L_f^2 \alpha}{\sqrt{K}} + \frac{3\rho\lambda(L_f + L_\omega)^2(\tau_{\sigma^2} + 2\bar{\tau} + 1)\alpha^2}{K} \right],$$

where  $D = \psi_{1/\rho}(x^1) - \psi(x^*)$ .

*Remark 4.* **Theorem 1** states a convergence rate of

$$\mathbb{E}[\|\nabla\psi_{1/\rho}(x^{k*})\|^2] = \mathcal{O}\left(\frac{1}{\sqrt{K}} + \frac{\bar{\tau}}{K} + \frac{\tau_{\sigma^2}}{K}\right),$$

where delay appears in a higher-order term compared to the conventional DSGD. The hyper-parameter  $\alpha$  balances optimality and noise. Larger  $\alpha$ , thus more aggressive stepsize, improves the first term at risk of making noise and delay-related terms worse. In practice, we can tune the stepsize to reach a proper trade-off.

Now that we have shown convergence of DSPL, it's desirable to see if practical acceleration techniques for SPL also apply in presence of delay. In the next section, we propose a momentum variant of DSPL and record it as DSEPL.

## 4 Extrapolated DSPL Method

In this section, we incorporate the extrapolation technique into the delayed prox-linear algorithm (DSEPL). Namely, before the master performs the proximal update, it uses two recent iterates to compute an extrapolated iterate  $y^k$ . Then a proximal update is done centered around  $y^k$  with delayed information. We summarize the procedure in **Algorithm 2**.

---

### Algorithm 2: Extrapolated DSPL

---

**Input:**  $x^1, x^0, \beta$ ;  
**for**  $k = 1, 2, \dots$  **do**  
    Let  $c(x^{k-\tau_k}, \xi^{k-\tau_k})$  and  $\nabla c(x^{k-\tau_k}, \xi^{k-\tau_k})$  be computed by a worker with delay  $\tau_k$ ;  
    In the master node update  

$$y^k = x^k + \beta(x^k - x^{k-1}),$$

$$x^{k+1} = \arg \min_x \{f_{x^{k-\tau_k}}(x, \xi^{k-\tau_k}) + \omega(x) + \frac{\gamma}{2}\|x - y^k\|^2\}.$$
  
**end**

---

To analyze the algorithm with extrapolation, we extend the framework from [12] to the delayed case and the analysis is based on an auxiliary iterate  $z^k := x^k + \beta\theta^{-1}(x^k - x^{k-1})$ , where the extrapolation parameter, also known as momentum, is fixed at some constant  $\beta \in [0, 1)$  and  $\theta = 1 - \beta$ . As extrapolation increases the instability of the iterations, we assume that delays are bounded.

**C1:** (Bounded delay) Delays are bounded by  $\tau < \infty$ .

Analysis of DSEPL uses a more complicated potential function developed in [26].

$$\psi_{1/\rho}(z^k) + \frac{\rho(\gamma\beta + \rho\beta^2\theta^{-2})}{2(\gamma - \lambda)\theta}\|x^k - x^{k-1}\|^2 \quad (5)$$

The following lemma presents a similar descent property for the potential function.

**Lemma 2.** Under **A1** to **A3** as well as **B1**, given  $0 \leq \beta < 1, \rho \geq 3\lambda + 2\kappa\beta + \kappa$  and  $\gamma > \rho$ , then

$$\begin{aligned} & \frac{(\rho - \kappa\theta)}{2\rho(\gamma - \kappa)\theta} \|\nabla\psi_{1/\rho}(z^k)\|^2 \\ & \leq \psi_{1/\rho}(z^k) - \mathbb{E}_k[\psi_{1/\rho}(z^{k+1})] + \frac{\rho\beta}{(\gamma - \kappa)\theta^2} \{\psi(x^k) - \mathbb{E}_k[\psi(x^{k+1})]\} \\ & \quad + \frac{\rho(2\rho\beta^2\theta^{-1} + \gamma\beta\theta)}{2(\gamma - \kappa)\theta^2} \{\|x^k - x^{k-1}\|^2 - \mathbb{E}_k[\|x^{k+1} - x^k\|^2]\} \\ & \quad + \frac{2\rho L_f^2}{(\gamma - \kappa)^2\theta^2} - \frac{\rho(\gamma\theta^2 - 2\theta(\rho + \kappa\beta) - 2\rho\beta^2\theta^{-1})}{2(\gamma - \kappa)\theta^2} \mathbb{E}_k[\|x^{k+1} - x^k\|^2] + \frac{\rho\mathbb{E}_k[\varepsilon_k]}{(\gamma - \kappa)\theta^2}, \end{aligned}$$

where  $\varepsilon_k = (\lambda\theta + \frac{\lambda}{2})\|x^{k+1} - x^{k-\tau_k}\|^2 + \frac{\lambda(1-\theta)}{2}\|x^k - x^{k-\tau_k}\|^2$  characterizes the error of delay.

We next bound the stochastic delay using **C1**.

**Lemma 3.** Under the same conditions as **Lemma 2** and **C1**, given  $\gamma > \max\{\rho, 2(\rho + \kappa\beta)\theta^{-1} + 2\rho\beta^2\theta^{-3}\}$ , then

$$\mathbb{E}[\|\nabla\psi_{1/\rho}(z^{k^*})\|^2] \leq \frac{2\rho\theta}{\rho - \kappa\theta} \left[ \frac{(\gamma - \kappa + \rho\beta\theta^{-2})D}{K} + \frac{2\rho L_f^2}{(\gamma - \kappa)\theta^2} + \frac{\rho\lambda(3\tau^2 + 2\beta)}{2\theta^2 K} \sum_{k=1}^K \mathbb{E}_k[\|x^{k+1} - x^k\|^2] \right],$$

where  $D = \max\{\psi_{1/\rho}(z^1) - \psi_{1/\rho}(z^*), \psi(x^1) - \psi(x^*)\}$ .

*Remark 5.* **Lemma 3** reveals the effect of extrapolation on the delayed algorithm. We notice that after simplification  $\theta = 1 - \beta$  appears in the denominator of the error from delay and will enlarge such an error if  $\beta \rightarrow 1$ . This is intuitive since when extrapolating using two iterations generated from delayed information, the error may be magnified.

By taking less aggressive steps, we bound the term  $\sum_{k=1}^K \mathbb{E}[\|x^{k+1} - x^k\|^2]$  and arrive at the final convergence result for DSEPL.

**Theorem 2.** Under the same conditions as **Lemma 3**, if we further choose  $\gamma \geq 2\theta^{-1}(\rho + \kappa\beta) + 2\rho\theta^{-3}\beta^2 + 2\lambda\theta^{-2}\beta + 3\lambda\theta^{-1}\tau^2$ , then

$$\mathbb{E}[\|\nabla\psi_{1/\rho}(z^{k^*})\|^2] \leq \frac{2\rho\theta}{(\rho - \kappa\theta)\sqrt{K}} \left( \frac{\lambda(3\tau^2 + 2\beta)}{\Gamma} + 1 \right) \left[ \frac{(\gamma - \kappa + \rho\beta\theta^{-2})D}{\sqrt{K}} + \frac{2\rho L_f^2\sqrt{K}}{(\gamma - \kappa)\theta^2} \right],$$

where  $\Gamma := \gamma\theta^2 - 2\theta(\rho + \kappa\beta) - 2\rho\beta^2\theta^{-1} - 3\lambda\tau^2 - 2\lambda\beta$ .

*Remark 6.* If  $\gamma = \mathcal{O}(\sqrt{K})$ , then  $\frac{(\gamma - \kappa + \rho\beta\theta^{-2})D}{K} + \frac{2\rho L_f^2}{(\gamma - \kappa)\theta^2} = \mathcal{O}(\frac{1}{\sqrt{K}})$ ,  $\Gamma^{-1} = \mathcal{O}(\frac{1}{\sqrt{K}})$  and

$$\mathbb{E}[\|\nabla\psi_{1/\rho}(z^{k^*})\|^2] = \mathcal{O}\left(\frac{1}{K} + \frac{1}{\sqrt{K}} + \left(\frac{1}{K} + \frac{1}{\sqrt{K}}\right)\frac{\tau^2}{\sqrt{K}}\right),$$

which implies that the delay is negligible if  $\tau = o(K^{1/4})$ .

*Remark 7.* Although our convergence result is based on the extrapolated sequence, we can leverage **Lemma 2** to show that  $\mathbb{E}[\|x^{k^*+1} - x^{k^*}\|^2]$ , and subsequently  $\mathbb{E}[\|z^{k^*} - x^{k^*}\|^2]$  is  $\mathcal{O}(\frac{1}{K})$ . Using the Lipschitz smoothness of the Moreau envelope, we have  $\mathbb{E}[\|\nabla\psi_{1/\rho}(x^{k^*})\|^2]$  is  $\mathcal{O}(\frac{1}{\sqrt{K}})$ .

After completing the analysis of DSPL and DSEPL, we take a look back at the aforementioned stochastic proximal subgradient-based methods, DSGD. It turns out the analysis tools we developed in the previous sections also benefit the subgradient-based methods and improve their convergence.

## 5 Delayed (Proximal) SGD

In this section, we leverage the tools developed in the previous sections to analyze a basic delayed stochastic proximal subgradient method (DSGD). Recall that DSGD method finds  $x^{k+1}$  iteratively by solving

$$\min_x \{ \langle g^{k-\tau_k}, x - x^k \rangle + \omega(x) + \frac{\gamma_k}{2} \|x - x^k\|^2 \}. \quad (6)$$

This framework is most frequently analyzed in the literature on delayed stochastic methods in a centralized architecture. To show the convergence of DSGD, we need to restrict  $f$  to a conventional setting of Lipschitzness

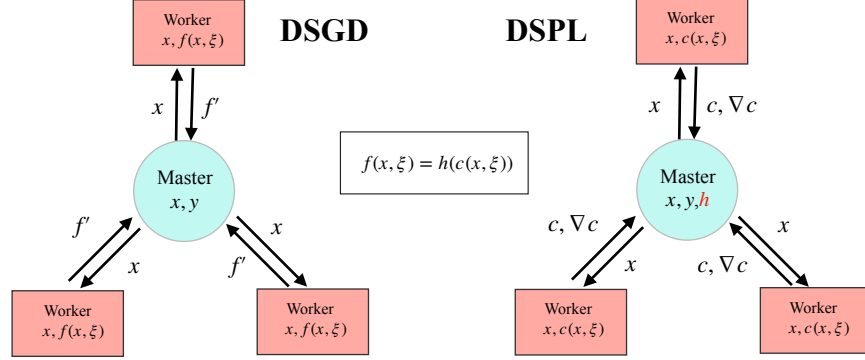


Figure 1: DSGD and DSPL in a master-worker architecture.

and make the following assumption.

**D1:**  $f(x, \xi)$  is  $L_f$ -Lipschitz continuous in  $\text{dom } \omega$  and  $\lambda$ -weakly convex for all  $\xi \sim \Xi$ .

Similar to the convergence analysis of DSPL, DSGD has the following descent property.

**Lemma 4.** Under **A1** to **A3** as well as **D1**, if  $\rho > 2\lambda + \kappa$ ,  $\gamma_k \geq \rho$ , then

$$\begin{aligned} \frac{\rho(\rho - 2\lambda - \kappa)}{2(\gamma_k - 2\lambda - \kappa)} \|\hat{x}^k - x^k\|^2 &\leq \psi_{1/\rho}(x^k) - \mathbb{E}_k[\psi_{1/\rho}(x^{k+1})] \\ &\quad + \frac{\rho\lambda}{\gamma_k - 2\lambda - \kappa} \mathbb{E}_k[\|x^{k+1} - x^{k-\tau_k}\|^2] + \frac{2\rho L_f}{\gamma_k - 2\lambda - \kappa} \mathbb{E}_k[\|x^{k+1} - x^{k-\tau_k}\|]. \end{aligned}$$

*Remark 8.* It is interesting to compare **Lemma 4** and **Lemma 1**, where in the result for DSPL, the dominating first order error  $\|x^{k+1} - x^{k-\tau_k}\|$  is replaced by a delay-free term. This difference explains why DSPL enjoys a better convergence rate technically.

Next, we develop the convergence of DSGD in **Theorem 3**.

**Theorem 3.** Under the same conditions as **Lemma 4** and letting **A4** hold, taking  $\gamma = 2\lambda + \kappa + \sqrt{K}/\alpha > \rho$  for some  $\alpha > 0$ , letting  $k^*$  be uniformly chosen between 1 and  $K$ ,

$$\mathbb{E}[\|\nabla \psi_{1/\rho}(x^{k^*})\|^2] \leq \frac{2\rho}{\rho - 2\lambda - \kappa} \left[ \frac{D}{\sqrt{K}\alpha} + \frac{2\sqrt{2}\rho L_f(L_f + L_\omega)\bar{\tau}\alpha}{\sqrt{K}} + \frac{2\rho\lambda(L_f + L_\omega)^2(\tau_{\sigma^2} + 2\bar{\tau} + 1)\alpha^2}{K} \right],$$

where  $D = \psi_{1/\rho}(x^1) - \psi(x^*)$ .

*Remark 9.* We note that the bound for DSGD states that

$$\mathbb{E}[\|\nabla \psi_{1/\rho}(x^{k^*})\|^2] = \mathcal{O}\left(\frac{\bar{\tau}}{\sqrt{K}} + \frac{\tau_{\sigma^2}}{K}\right).$$

Although delay appears in the dominating term, its impact is less significant compared to the previous  $\mathcal{O}(\frac{\tau}{\sqrt{K}})$  result [38] since  $\bar{\tau}$  is often much smaller than  $\tau$ .



Our results also improve the convergence rate of DSGD assuming that  $f(x, \xi)$  is  $\lambda$ -smooth.

**Theorem 4.** *Under the same conditions as Lemma 4, letting A4 hold and further assuming that  $f$  is  $\lambda$ -smooth. If we take  $\gamma = 2\lambda + \kappa + \sqrt{K}/\alpha > \rho$  for some  $\alpha > 0$ , letting  $k^*$  be uniformly chosen between 1 and  $K$ , we have*

$$\mathbb{E}[\|\nabla\psi_{1/\rho}(x^{k^*})\|^2] = \mathcal{O}\left(\frac{1}{\sqrt{K}} + \frac{\bar{\tau}}{K} + \frac{\tau_{\sigma^2}}{K}\right). \quad (7)$$

*Remark 10.* Following exactly the same argument as Theorem 4, we can also show that in the proximal setting, DSEGD, namely the momentum variant of DSGD, has  $\mathcal{O}(\frac{1}{K} + \frac{1}{\sqrt{K}} + (\frac{1}{K} + \frac{1}{\sqrt{K}})\frac{\tau_{\sigma^2}}{\sqrt{K}})$  rate of convergence.

**DSPL vs. DSGD** Using the example of composition function (2), we give some intuition why DSPL outperforms DSGD. Figure 1 illustrates the architecture of compared algorithms. Intuitively, as the stochastic algorithm converges, we have  $\lim_{k \rightarrow 0} \|x^k - x^{k+1}\| = 0$ . For simplicity, we assume in Algorithm 1 that both function value  $c(x, \xi)$  and gradient  $\nabla c(x, \xi)$  are Lipschitz continuous. When  $x^k \approx x^{k-\tau_k}$ , DSPL enjoys an increasingly stable estimation of the proximal mapping (4), as the influence of delay is diminishing and the error is mainly driven by stochastic sampling. The same conclusion holds on smooth DSGD due to the Lipschitz continuity of  $\nabla f$ . On the other hand, when DSGD is applied for nonsmooth weakly convex problems, the master node receives an out-of-date subgradient  $f'$  from the worker and solves (6). However, due to the nonsmoothness of  $f$ ,  $f'$  may vary significantly at the iterates even when the sequence converges:  $\lim_{k \rightarrow 0} \|x^k - x^{k+1}\| = 0$ . Hence, DSGD will constantly suffer from delay throughout the whole optimization procedure.

## 6 Experiments

This section conducts numerical studies on the **robust phase retrieval** problem to demonstrate the efficiency of our proposed methods. Numerical studies on **blind deconvolution** are given in the appendix. Given a measuring matrix  $A \in \mathbb{R}^{m \times n}$  and a set of observations  $b_i \approx |\langle a_i, x^* \rangle|^2, 1 \leq i \leq m$ , robust phase retrieval aims to recover the true signal from the following optimization problem

$$\min_{x \in \mathbb{R}^n} \frac{1}{m} \sum_{i=1}^m |\langle a_i, x \rangle|^2 - b_i| + \mathbb{I}\{\|x\| \leq \Delta\},$$

where  $\mathbb{I}\{\cdot\}$  denotes the indicator function and  $\ell_1$  loss function is used to improve recovery robustness. Our experiment contains two parts. The first part follows [38], where the algorithms are profiled in a real asynchronous environment implemented via MPI. Additionally, to investigate the robustness of the algorithms against delays more accurately, our second experiment is run sequentially with simulated delays from various distributions. We present the detailed setup as follows.

### 6.1 Experiment Setup

**Synthetic Data.** For the synthetic data, we take  $m = 300, n = 100$  in the experiments of simulated delay and  $m = 1500, n = 300$  in the asynchronous environment. The data generation follows the setup of [12], where, given some conditioning parameter  $\kappa \geq 1$ , we compute  $A = QD, Q \in \mathbb{R}^{m \times n}, q_{ij} \sim \mathcal{N}(0, 1)$  and  $D = \text{diag}(d), d \in \mathbb{R}^n, d_i \in [1/\kappa, 1], \forall i$ . Then we generate a true signal  $x^* \sim \mathcal{N}(0, I)$  and obtain the measurements  $b$  using formula  $b_i = \langle a_i, x \rangle^2$ . Last we randomly choose  $p_{\text{fail}}$ -fraction of the measurements and add  $\mathcal{N}(0, 25)$  to them to simulate corruption.

**Real-life Data.** The real-life data is generated from **zipcode** dataset, where we vectorize a true  $16 \times 16$  hand-written digit from [18] and use it as the signal. The measuring matrix  $A$  comes from a normalized Hadamard matrix  $H \in \mathbb{R}^{256 \times 256}$ : we generate three diagonal matrices  $S_j = \text{diag}(s_j), j = 1, 2, 3$  where each element of  $s \in \mathbb{R}^{256}$  is taken from  $\{-1, 1\}$  randomly and we let  $A = H[S_1, S_2, S_3]^T \in \mathbb{R}^{768 \times 256}$ . Similar to the synthetic data, we corrupt  $p_{\text{fail}}$  fraction of the measurements by setting them to 0.

- 1) **Dataset.** In the asynchronous environment, we keep up with [38] setting  $\kappa = 1, p_{\text{fail}} = 0$  and in the simulated environment, we follow [12] setting  $\kappa \in \{1, 10\}$  and  $p_{\text{fail}} \in \{0.2, 0.3\}$ .
- 2) **Initial Point and Radius.** For the synthetic data, we generate  $x' \sim \mathcal{N}(0, I_n)$  and start from  $x^0 = x^1 = \frac{x'}{\|x'\|}$  and for `zipcode` data, we generate  $x' \sim \mathcal{N}(x^*, I_n)$  and take  $x^0 = x^1 = x'$ .  $\Delta = 1000\|x^0\|$ .
- 3) **Stopping Criterion.** We allow all the algorithms to run 400 epochs, i.e.,  $K = 400m$ . In the asynchronous environment, algorithms run until reaching the maximum iteration number. In the simulated environment, algorithms stop if  $f$  falls below  $1.5f(x^*)$ . Since  $f$  might contain corrupted measurements,  $f(x^*) \geq 0$ .
- 4) **Stepsize.** We tune the stepsize parameter setting  $\gamma = \sqrt{K/\alpha}$ , where  $\alpha \in \{0.1, 0.5, 1.0\}$  in the asynchronous environment,  $\alpha \in [10^{-2}, 10^1]$  for synthetic data in the simulated environment and  $\alpha \in [10^0, 10^1]$  for the `zipcode` dataset.
- 5) **Momentum Parameter.** In the asynchronous environment, we allow  $\beta \in \{0, 0.1, 0.3, 0.6\}$  and in the simulated environment, we test  $\beta \in \{0.6, 0.9\}$  for the synthetic and `zipcode` data respectively.
- 6) **Simulated Delay.** In the simulated environment, we generate  $\tau_k$  from two common distributions from literature, which are geometric  $\mathcal{G}(p)$  and Poisson  $\mathcal{P}(\lambda)$  [42]. After the delay is generated, it is truncated by twice the mean of the distribution to impose boundedness staleness.
- 7) **Trade-off between Computation and Communication.** In the asynchronous environment, the numerical linear algebra on the worker uses a raw implementation (not importing package) to balance the cost of gradient computation and communication.

## 6.2 Asynchronous Environment

The first part of our experiment runs in an asynchronous environment implemented via an MPI interface of Python and is profiled on an Intel(R) Xeon(R) CPU E5-2640 v4 @ 2.40GHz machine with 10 cores and 20 threads. We note that the experiment is run on a single machine to verify our theoretical analysis rather than to test the algorithm's real performance on a specific distributed architecture.

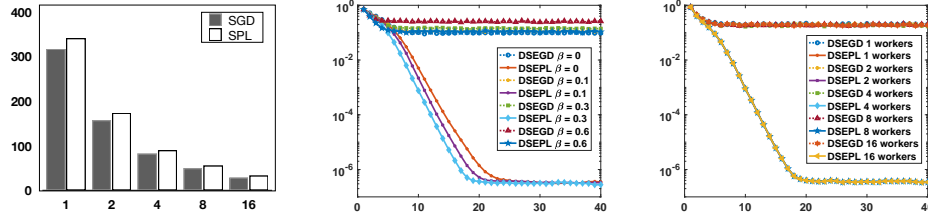


Figure 2: First: speedup in time and the number of workers. Second: progress of  $\|x^k - x^*\|$  in the first 40 epochs given 16 workers and  $\alpha = 0.5$ . Third: progress of  $f(x^k) - f(x^*)$  in the first 40 epochs given  $\beta = 0.3$  and different number of workers.

The first figure plots the wall-clock time (in seconds) for DSPL(DSEPL) and DSGD(DSEGD) to complete 400 epochs as the number of workers increases. It is observed that both algorithms exhibit remarkable speed-up with more workers. We also note that DSPL takes slightly more time than DSGD due to the extra need to pass the function value to the master. But as the second figure suggests, such an extra cost is justified by the faster convergence behavior. More specifically, we observe that in the first several epochs DSPL and DSEPL reach a high accuracy of  $10^{-6}$  in both function value and distance to the optimal solution, while DSGD and DSEGD stagnate by a relatively low-accuracy solution of  $10^{-2}$ . These observations suggest that DSPL offers better convergence behavior than the methods only based on subgradient. Our next experiment investigates the robustness of algorithms against delays and as the third figure suggests, both DSPL(DSEPL) and DSGD(DSEGD) are insensitive to the increase in the number of workers and this further validates their use in practice.

### 6.3 Simulated Environment

The second part of our experiment is based on the simulated delay, where the algorithm runs sequentially but the gradient information is computed from previous iterates.

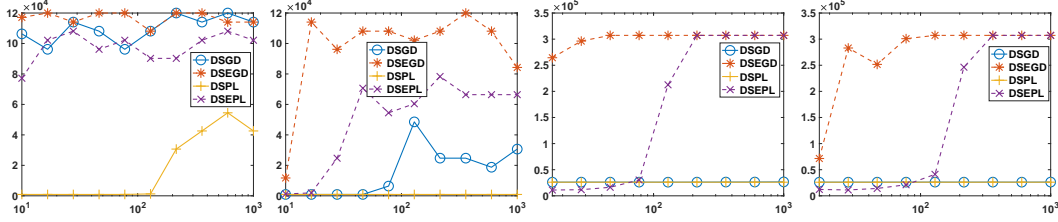


Figure 3: Left to right:  $(\kappa, p_{\text{fail}}) = (10, 0.3), \alpha = 5.0$ , Geometric and Poisson delays; **zipcode** data of  $p_{\text{fail}} = 0.2, \alpha = 6.0$ , Geometric and Poisson delays. x-axis represents  $\tau$  and y-axis shows average iteration number to reach the stopping criterion over 20 tests.

Figure 3 plots the impact of staleness on the number of iterations each algorithm takes to reach the desired accuracy. It can be seen that with other parameters fixed, DSPL tends to be more robust against delays than the pure subgradient-based methods, which is consistent with the theoretical results. Moreover, we observe that when extrapolation is used, the algorithm converges faster at the cost of less robustness as delay increases.

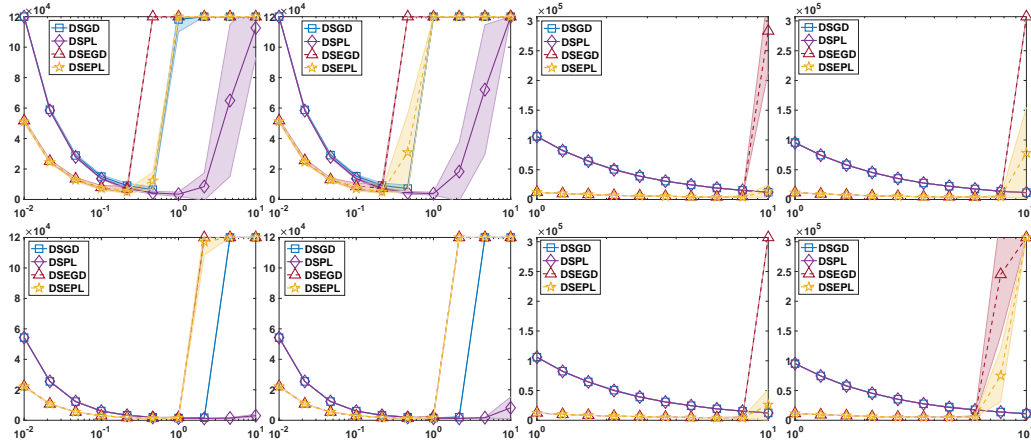


Figure 4: First row(Geometric) left:  $(\kappa, p_{\text{fail}}) = (1, 0.3), \beta = 0.6, \tau \in \{28, 47\}$ , right: **zipcode**  $p_{\text{fail}} = 0.3, \beta = 0.9, \tau \in \{28, 600\}$ . Second row(Poisson) left:  $(\kappa, p_{\text{fail}}) = (10, 0.2), \beta = 0.6, \tau \in \{28, 47\}$ . right: **zipcode**  $p_{\text{fail}} = 0.3, \beta = 0.9, \tau \in \{28, 600\}$ .

Our last experiment investigates the robustness of DSPL compared to DSGD and justifies the use of extrapolation in presence of delay. Figure 4 plots the number of iterations for each algorithm to converge with different datasets, extrapolation parameters, and delays. In spite of delays, DSPL and DSEPL still admit a wider range of stepsize parameters ensuring convergence than DSGD. Also, when the stepsize is not large, the use of extrapolation can effectively accelerate the convergence.

## 7 Conclusions

For distributed optimization of a class of structured nonsmooth nonconvex problems, we present a new algorithm DSPL and its momentum variant DSEPL as better alternatives to the conventional subgradient-based methods. By exploiting the composite structure of the objective, we show that the prox-linear methods have an attractive property in that the asynchronous delay is negligible. While we focus on developing new distributed algorithms, our technique facilitates an improved analysis of DSGD by reducing the dependence on maximum delay to expected delay. One future direction is to apply the prox-linear methods to more distributed environments. For example, it would be interesting to further extend the prox-linear methods to optimization in decentralized networks.

## References

- [1] A. Agarwal and J. C. Duchi. Distributed delayed stochastic optimization. In J. Shawe-Taylor, R. Zemel, P. Bartlett, F. Pereira, and K. Weinberger, editors, *Advances in Neural Information Processing Systems*, volume 24. Curran Associates, Inc., 2011.
- [2] Y. Arjevani, O. Shamir, and N. Srebro. A tight convergence analysis for stochastic gradient descent with delayed updates. In *Algorithmic Learning Theory*, pages 111–132. PMLR, 2020.
- [3] K. Bäckström, M. Papatriantafilou, and P. Tsigas. Mindthestep-asynpcsgd: Adaptive asynchronous parallel stochastic gradient descent. In *2019 IEEE International Conference on Big Data (Big Data)*, pages 16–25. IEEE, 2019.
- [4] D. Bertsekas and J. Tsitsiklis. *Parallel and distributed computation: numerical methods*. Athena Scientific, 2015.
- [5] V. Charisopoulos, Y. Chen, D. Davis, M. Díaz, L. Ding, and D. Drusvyatskiy. Low-rank matrix recovery with composite optimization: good conditioning and rapid convergence. *Foundations of Computational Mathematics*, 21(6):1505–1593, 2021.
- [6] S. Chen, A. Garcia, and S. Shahrampour. On distributed non-convex optimization: Projected subgradient method for weakly convex problems in networks. *IEEE Transactions on Automatic Control*, 2021.
- [7] A. Cohen, A. Daniely, Y. Drori, T. Koren, and M. Schain. Asynchronous stochastic optimization robust to arbitrary delays. *Advances in Neural Information Processing Systems*, 34, 2021.
- [8] D. Davis and D. Drusvyatskiy. Stochastic model-based minimization of weakly convex functions. *SIAM Journal on Optimization*, 29(1):207–239, 2019.
- [9] D. Davis and D. Drusvyatskiy. Stochastic model-based minimization of weakly convex functions. *SIAM Journal on Optimization*, 29(1):207–239, 2019.
- [10] D. Davis and D. Drusvyatskiy. Graphical convergence of subgradients in nonconvex optimization and learning. *Mathematics of Operations Research*, 47(1):209–231, 2022.
- [11] D. Davis, D. Drusvyatskiy, and K. J. MacPhee. Stochastic model-based minimization under high-order growth. *arXiv preprint arXiv:1807.00255*, 2018.
- [12] Q. Deng and W. Gao. Minibatch and momentum model-based methods for stochastic weakly convex optimization. *Advances in Neural Information Processing Systems*, 34, 2021.
- [13] D. Drusvyatskiy and C. Paquette. Efficiency of minimizing compositions of convex functions and smooth maps. *Mathematical Programming*, pages 1–56, 2018.

- [14] J. C. Duchi and F. Ruan. Stochastic methods for composite and weakly convex optimization problems. *SIAM Journal on Optimization*, 28(4):3229–3259, 2018.
- [15] J. C. Duchi and F. Ruan. Solving (most) of a set of quadratic equalities: Composite optimization for robust phase retrieval. *Information and Inference: A Journal of the IMA*, 8(3):471–529, 2019.
- [16] H. R. Feyzmahdavian, A. Aytakin, and M. Johansson. A delayed proximal gradient method with linear convergence rate. In *2014 IEEE International Workshop on Machine Learning for Signal Processing (MLSP)*, pages 1–6. IEEE, 2014.
- [17] R. Fletcher. A model algorithm for composite nondifferentiable optimization problems. In *Nondifferential and Variational Techniques in Optimization*, pages 67–76. Springer, 1982.
- [18] T. Hastie, R. Tibshirani, J. H. Friedman, and J. H. Friedman. *The elements of statistical learning: data mining, inference, and prediction*, volume 2. Springer, 2009.
- [19] S. P. Karimireddy, Q. Rebjock, S. Stich, and M. Jaggi. Error feedback fixes signsgd and other gradient compression schemes. In *International Conference on Machine Learning*, pages 3252–3261. PMLR, 2019.
- [20] A. S. Lewis and S. J. Wright. A proximal method for composite minimization. *Mathematical Programming*, 158(1):501–546, 2016.
- [21] X. Li, Z. Zhu, A. M.-C. So, and J. D. Lee. Incremental methods for weakly convex optimization. *arXiv preprint arXiv:1907.11687*, 2019.
- [22] X. Lian, Y. Huang, Y. Li, and J. Liu. Asynchronous parallel stochastic gradient for nonconvex optimization. *Advances in Neural Information Processing Systems*, 28, 2015.
- [23] X. Lian, C. Zhang, H. Zhang, C.-J. Hsieh, W. Zhang, and J. Liu. Can decentralized algorithms outperform centralized algorithms? a case study for decentralized parallel stochastic gradient descent. *Advances in Neural Information Processing Systems*, 30, 2017.
- [24] X. Lian, W. Zhang, C. Zhang, and J. Liu. Asynchronous decentralized parallel stochastic gradient descent. In *International Conference on Machine Learning*, pages 3043–3052. PMLR, 2018.
- [25] H. Lu. "relative continuity" for non-lipschitz nonsmooth convex optimization using stochastic (or deterministic) mirror descent. *INFORMS Journal on Optimization*, 1(4):288–303, 2019.
- [26] V. Mai and M. Johansson. Convergence of a stochastic gradient method with momentum for non-smooth non-convex optimization. In *International Conference on Machine Learning*, pages 6630–6639. PMLR, 2020.
- [27] B. McMahan and M. Streeter. Delay-tolerant algorithms for asynchronous distributed online learning. *Advances in Neural Information Processing Systems*, 27, 2014.
- [28] K. Mishchenko, F. Bach, M. Even, and B. Woodworth. Asynchronous SGD beats minibatch SGD under arbitrary delays. In A. H. Oh, A. Agarwal, D. Belgrave, and K. Cho, editors, *Advances in Neural Information Processing Systems*, 2022.
- [29] A. Nedić, D. P. Bertsekas, and V. S. Borkar. Distributed asynchronous incremental subgradient methods. *Studies in Computational Mathematics*, 8(C):381–407, 2001.
- [30] A. Nemirovski, A. Juditsky, G. Lan, and A. Shapiro. Robust stochastic approximation approach to stochastic programming. *SIAM Journal on Optimization*, 19(4):1574–1609, 2009.
- [31] B. Recht, C. Re, S. Wright, and F. Niu. Hogwild!: A lock-free approach to parallelizing stochastic gradient descent. volume 24, 2011.

- [32] H. Robbins and S. Monro. A stochastic approximation method. *The Annals of Mathematical Statistics*, pages 400–407, 1951.
- [33] R. T. Rockafellar. Convex analysis princeton university press. *Princeton, NJ*, 1970.
- [34] S. Shalev-Shwartz, O. Shamir, N. Srebro, and K. Sridharan. Stochastic convex optimization. In *COLT*, volume 2, page 5, 2009.
- [35] S. Sra, A. W. Yu, M. Li, and A. Smola. Adadelat: Delay adaptive distributed stochastic optimization. In *Artificial Intelligence and Statistics*, pages 957–965. PMLR, 2016.
- [36] S. U. Stich and S. P. Karimireddy. The error-feedback framework: Better rates for sgd with delayed gradients and compressed updates. *Journal of Machine Learning Research*, 21:1–36, 2020.
- [37] I. Sutskever, J. Martens, G. Dahl, and G. Hinton. On the importance of initialization and momentum in deep learning. In *International Conference on Machine Learning*, pages 1139–1147, 2013.
- [38] Y. Xu, Y. Xu, Y. Yan, and J. Chen. Distributed stochastic inertial-accelerated methods with delayed derivatives for nonconvex problems. *SIAM Journal on Imaging Sciences*, 15(2):550–590, 2022.
- [39] J. Zeng and W. Yin. On nonconvex decentralized gradient descent. *IEEE Transactions on signal processing*, 66(11):2834–2848, 2018.
- [40] J. Zhang and L. Xiao. Stochastic variance-reduced prox-linear algorithms for nonconvex composite optimization. *Mathematical Programming*, pages 1–43, 2021.
- [41] S. Zhang and N. He. On the convergence rate of stochastic mirror descent for nonsmooth nonconvex optimization. *arXiv preprint arXiv:1806.04781*, 2018.
- [42] W. Zhang, S. Gupta, X. Lian, and J. Liu. Staleness-aware async-sgd for distributed deep learning. *arXiv preprint arXiv:1511.05950*, 2015.
- [43] S. Zheng, Q. Meng, T. Wang, W. Chen, N. Yu, Z.-M. Ma, and T.-Y. Liu. Asynchronous stochastic gradient descent with delay compensation. In *International Conference on Machine Learning*, pages 4120–4129. PMLR, 2017.

# Appendix

## Table of Contents

---

<b>A</b>	<b>More on the Related Works</b>	<b>16</b>
<b>B</b>	<b>Convergence Analysis of DSPL</b>	<b>16</b>
B.1	Bregman Divergence . . . . .	16
B.2	Auxiliary Lemmas . . . . .	17
B.3	Preliminaries and analysis of Bregman DSPL . . . . .	18
B.4	Proof of Main Results in Section 3 . . . . .	23
B.5	Kernel and Subproblems . . . . .	23
<b>C</b>	<b>Convergence Analysis of DSEPL</b>	<b>25</b>
C.1	Auxiliary Results . . . . .	25
C.2	Proof of Lemma 2 . . . . .	26
C.3	Proof of Lemma 3 . . . . .	29
C.4	Proof of Theorem 2 . . . . .	31
<b>D</b>	<b>Improved Analysis of DSGD</b>	<b>31</b>
D.1	Proof of Lemma 4 . . . . .	31
D.2	Proof of Theorem 3 . . . . .	33
D.3	Proof of Theorem 4 . . . . .	34
<b>E</b>	<b>Additional Experiments</b>	<b>34</b>
E.1	Experiment Setup . . . . .	34
E.2	Asynchronous Environment . . . . .	34
E.3	Simulated Environment . . . . .	34
E.4	Proximal Sub-problems . . . . .	35

---

**Structure of the Appendix** The appendix is organized as follows. In Section A, we review some other related works. In Section B, we present a more general Bregman DSPL which relaxes the Lipschitzness assumption on the objective. The convergence result of standard DSPL immediately follows from our more general argument. In Section C and Section D, we present the convergence analysis of DSEPL and DSGD, respectively. In Section E, we display the additional experiment results on the blind deconvolution problem.

## A More on the Related Works

First, we review the literature on stochastic weakly-convex optimization. The Prox-Linear (PL) method [20, 13, 17] has received more attention lately. The seminal work Davis and Drusvyatskiy [8] conducts a novel complexity analysis using Moreau envelope as the potential function. They show that SGD (and many other stochastic algorithms) achieves an  $\mathcal{O}(\frac{1}{\varepsilon^4})$  complexity in terms of convergence to the proximity of approximate stationary points. Li et al. [21] analyzes an incremental subgradient method for finite-sum problems. Zhang and Xiao [40] extends the prox-linear algorithm to the finite-sum setting and provides analysis based on variance-reduction. SGD with momentum is studied in Mai and Johansson [26] and Deng and Gao [12] reveals that SPL can be accelerated using minibatches even in the presence of nonsmooth objective functions. Deng and Gao [12] also employs heavy-ball momentum to further improve the model-based optimization.

There is substantial literature on distributed and asynchronous optimization. We refer to the seminal work Bertsekas and Tsitsiklis [4]. In addition to the aforementioned asynchronous issues, another important research direction concerns reducing the network communication cost by gradient compression. For example, see Karimireddy et al. [19]. Besides the centralized setting, there is also growing interest in decentralized algorithms. Recently, Chen et al. [6] presents a decentralized SGD in the network where nodes exchange parameters and subgradients locally. However, their method requires all the nodes to update synchronously and only proves asymptotic convergence of SGD. An extensive study of decentralized optimization is beyond our work. Therefore, we refer interested readers to [23, 24, 39] for more recent advances.

## B Convergence Analysis of DSPL

In this section, we introduce a more general DSPL associated with Bregman divergence and establish its convergence analysis. A great advantage of this approach is that by using appropriate divergence function, we can handle models where Lipschitz continuity of  $c(x, \xi)$  in B1 does not hold. Section B.1 introduces Bregman divergence, which generalizes the Euclidean distance using kernel functions. Section B.2 presents some auxiliary results for our proof. We develop the convergence analysis of Bregman DSPL in Section B.3. The convergence analysis of DSPL is given in Section B.4. Finally, Section B.5 discusses some technical issues in solving the Bregman proximal subproblem.

### B.1 Bregman Divergence

Given a Legendre function  $d(\cdot)$  [33] that is proper, closed, strictly convex and essentially smooth, it induces the Bregman divergence defined by

$$V_d(x, y) := d(x) - d(y) - \langle \nabla d(y), x - y \rangle$$

and  $d$  is denoted as the kernel of  $V_d$ . Since  $d$  is strictly convex, we have  $V_d(x, y) \geq 0$  and the equality holds if and only if  $x = y$ . The notion of Bregman divergence greatly enhances the coverage of the algorithms and has recently been adopted in the context of weakly convex optimization [41, 11] to tackle nonsmooth nonconvex optimization. In this paper, we mainly leverage the concept of relative Lipschitzness to extend the analysis of delayed stochastic algorithms. First we give their formal definitions.

**Definition 1.** (Relative Lipschitz continuity) [25]  $f : \mathbb{R}^n \rightarrow \mathbb{R}$  is  $L$ -relative continuous with respect to the kernel  $d$  if any  $x, y \in \text{dom } d$ ,  $x \neq y$

$$\sup_{g \in \partial f(x)} \|g\| \leq \frac{L\sqrt{2V_d(y, x)}}{\|y - x\|}$$

holds. Moreover, if  $f$  is differentiable over  $\text{dom } f$ , then

$$\|\nabla f(x)\| \leq \frac{L\sqrt{2V_d(y, x)}}{\|y - x\|}.$$



## Bregman Proximal Mapping and Bregman Envelope

As in conventional weakly convex optimization, we need an approximate measure of stationarity in non-Euclidean setting. A naturally choice is the Bregman envelope [11]. For any  $\rho > 0$ , the Bregman envelope of  $f$  with respect to kernel  $d$  is defined by

$$\psi_{1/\rho}^d(x) := \min_y \{f(y) + \omega(y) + \rho V_d(y, x)\}$$

and the Bregman proximal mapping is

$$\text{prox}_{\psi/\rho}^d(x) := \arg \min_y \{f(y) + \omega(y) + \rho V_d(y, x)\}.$$

For brevity we sometimes refer to  $\text{prox}_{\psi/\rho}^d(x)$  as  $\hat{x}$  and  $\mathbb{E}[V_d(\hat{x}^k, x^k)]$  has been proven a proper measure of the convergence of stochastic algorithms [11]. Particularly, in the Euclidean setting we have  $V_d(\hat{x}^k, x^k) = \frac{1}{2} \|\hat{x}^k - x^k\|^2 = \frac{1}{2\rho^2} \|\nabla \psi_{1/\rho}^d(x)\|^2$ . When the context is clear, we will use  $\psi = \psi^d$  directly if  $d(x) = \frac{1}{2} \|x\|^2$ .

## B.2 Auxiliary Lemmas

In this section, we present all the auxiliary lemmas that will be used in the proof of our main results. Some of them are well-known but for completeness, we reproduce them here.

First, we introduce the three-point lemma, which will be frequently used in our analysis.

**Lemma 5.** (Three point lemma). *Let  $f$  be a closed convex function and define*

$$z = \arg \min_x \{f(x) + \gamma V_d(x, y)\}.$$

*for some  $y \in \text{dom } d$ . Then we have*

$$f(z) + \gamma V_d(z, y) \leq f(x) + \gamma V_d(x, y) - \gamma V_d(x, z), \forall x \in \text{dom } d.$$

The next lemma bounds the size of a proximal step by the strong regularization and Lipschitzian property.

**Lemma 6.** (Bounding the proximal step) *Given divergence  $V_d$  generated by some 1-strongly convex function  $d$ , let  $f$  be  $L$ -relatively Lipschitz to  $d$ . For any  $\gamma > 0$ , if we define*

$$x^+ = \arg \min_y \{f(y) + \gamma V_d(y, x)\},$$

*then*

$$\sqrt{V_d(x^+, x)} \leq \sqrt{2\gamma}^{-1} L \tag{8}$$

*and*

$$\|x^+ - x\| \leq 2\gamma^{-1} L. \tag{9}$$

*Proof.* By the optimality of  $x^+$  and relative Lipschitzness, we have

$$f(x^+) + \gamma V_d(x^+, x) \leq f(x)$$

and

$$\gamma V_d(x^+, x) \leq f(x) - f(x^+) \leq L \sqrt{2V_d(x^+, x)}. \tag{10}$$

Dividing both sides of (10) by  $\sqrt{V_d(x^+, x)}$  gives (8) and (9) uses  $V_d(x^+, x) \geq \frac{1}{2} \|x^+ - x\|^2$ .  $\square$

---

**Algorithm 3:** A delayed stochastic prox-linear method with Bregman proximal updates

---

**Input:**  $x^1$ ;  
**for**  $k = 1, 2, \dots$  **do**  
    Let  $c(x^{k-\tau_k}, \xi^{k-\tau_k})$  and  $\nabla c(x^{k-\tau_k}, \xi^{k-\tau_k})$  be computed by a worker with delay  $\tau_k$ ;  
    In the master node update  
        
$$x^{k+1} = \arg \min_x \{h(c(x^{k-\tau_k}, \xi^k) + \langle \nabla c(x^{k-\tau_k}, \xi^k), x - x^k \rangle) + \omega(x) + \gamma_k V_d(x, x_k)\} \quad (11)$$
  
    **end**

---

### B.3 Preliminaries and analysis of Bregman DSPL

In this section, we present the convergence results of DSPL in a broader context of Bregman proximal mapping and our main results hold by taking the Euclidean kernel. As we mentioned in **Remark 2**, DSPL works replacing  $\frac{1}{2}\|\cdot\|^2$  regularization by divergence  $V_d$  and we summarize the update in **Algorithm 3**. Now we overload the assumptions used in **Section 3**.

- A1'**: (I.i.d. sample) It is possible to draw i.i.d. samples  $\{\xi^k\}$  from  $\Xi$ .
- A2'**: (Relative Lipschitz continuity)  $\omega(x)$  is  $L_\omega$  relatively Lipschitz continuous to  $d$ .
- A3'**: (Weak convexity)  $\omega(x)$  is  $\kappa$ -weakly convex.
- A4'**: (Strongly-convex kernel) Kernel function  $d$  is 1-strongly convex.
- A5'**: (Bounded moment) The distribution of the stochastic delays  $\{\tau_k\}$  has bound the first and second moments.  
i.e.,  $\mathbb{E}[\tau_k] \leq \bar{\tau} < \infty, \mathbb{E}[\tau_k^2] \leq \tau_{\sigma^2} < \infty, \forall k$ .
- B1'**:  $h(x)$  is convex and  $L_h$ -Lipschitz continuous;  $c(x, \xi)$  has  $C$ -Lipschitz continuous gradient and is  $L_c$ -relatively Lipschitz-continuous with respect to  $d$ ,  $\forall \xi \sim \Xi$ .

*Remark 11.* It can be seen that we added extra assumptions on the kernel and relaxed the Lipschitz continuity of  $c$  in **B1'** and  $\omega$  in **A3'**. Although the rest of the assumptions are exactly the same as in the Euclidean setting, for completeness we duplicate them here.

With the above assumptions, we can further derive a more general version of **Proposition 1**.

**Proposition 2** (**Proposition 1** in the Bregman setting).

- P1'**: (Convexity)  $f_z(x, \xi)$  is convex,  $\forall x, z \in \text{dom } d, \xi \sim \Xi$ .
- P2'**: (Two-sided approximation)  $|f_z(x, \xi) - f(x, \xi)| \leq \frac{L_h C}{2} \|x - z\|^2, \forall x, z \in \text{dom } d, \xi \sim \Xi$ .
- P3'**: (Relative Lipschitzness)

$$f_z(x, \xi) - f_z(y, \xi) \leq L_h L_c \sqrt{2V_d(y, x)}, \forall x, y, z \in \text{dom } d, \xi \sim \Xi$$

*Remark 12.* We note that slightly different from **Proposition 1**, we do not need  $\text{dom } d$  to be a bounded set.

As we do in **Section 3**, we take  $L_f = L_h L_c, \lambda = L_h C$  and use these constants to present the results. Our analysis adopts the conventional potential reduction framework but a more careful treatment of stochastic noise is needed to obtain an improved convergence result. The next lemma bounds the stochastic noise of the algorithm and is key to our improved convergence in DSPL.

**Lemma 7** (Stability of the stochastic iteration). *Assume that the assumptions **A1'** to **A4'** hold. If  $f_x(\cdot, \xi)$  is convex and  $L_f$ -relative Lipschitz to  $d$ , then the abstract proximal iteration*

$$x^{k+1} = \arg \min_x \{f_{x^{k-\tau_k}}(x, \xi^{k-\tau_k}) + \omega(x) + \gamma_k V_d(x, z^k)\}$$

*satisfies*

$$|\mathbb{E}_k \{ \mathbb{E}_\xi [f_{x^{k-\tau_k}}(x^{k+1}, \xi)] - f_{x^{k-\tau_k}}(x^{k+1}, \xi^{k-\tau_k}) \}| \leq \frac{2L_f^2}{\gamma_k - \kappa},$$

*for any  $\gamma_k > \kappa$ .*

Now we can get the lemmas that match our main results in a Bregman context.

**Lemma 8** (**Lemma 1** in the Bregman setting). *Assume that **A1'** to **A4'** as well as **B1'** holds, if we take  $\rho \geq 2\lambda + \kappa, \gamma_k \geq \rho$ , then*

$$\begin{aligned} \frac{\rho(\rho - 2\lambda - \kappa)}{\gamma_k - 2\lambda - \kappa} V_d(\hat{x}^k, x^k) &\leq \psi_{1/\rho}^d(x^k) - \mathbb{E}_k[\psi_{1/\rho}^d(x^{k+1})] \\ &\quad + \frac{3\rho\lambda}{2(\gamma_k - 2\lambda - \kappa)} \mathbb{E}_k[\|x^{k+1} - x^{k-\tau_k}\|^2] + \frac{2\rho L_f^2}{\gamma_k(\gamma_k - 2\lambda - \kappa)} \end{aligned}$$

**Theorem 5** (**Theorem 1** in the Bregman setting). *Assuming all the conditions of **Lemma 8**, taking  $\gamma = 2\lambda + \kappa + \sqrt{K}/\alpha > \rho$  for some  $\alpha > 0$  and letting  $k^*$  be an index chosen from  $\{1, \dots, K\}$  uniformly at random, we have*

$$\mathbb{E}[V_d(\hat{x}^{k^*}, x^{k^*})] \leq \frac{1}{\rho(\rho - 2\lambda - \kappa)} \left[ \frac{D}{\sqrt{K}\alpha} + \frac{2\rho L_f^2 \alpha}{\sqrt{K}} + \frac{3\rho\lambda(L_f + L_\omega)^2(\tau_{\sigma^2} + 2\bar{\tau} + 1)\alpha^2}{K} \right],$$

where  $D = \psi_{1/\rho}^d(x^1) - \psi(x^*)$ .

---

### Proof Proposition 2

---

$f_z(x, \xi)$  inherits convexity from  $h$ . The other properties hold by

$$\begin{aligned} &|f(x, \xi) - f_y(x, \xi)| \\ &= |h(c(x, \xi)) - h(c(y, \xi) + \langle \nabla c(y, \xi), x - y \rangle)| \\ &\leq L_h |c(x, \xi) - c(y, \xi) - \langle \nabla c(y, \xi), x - y \rangle| \\ &\leq \frac{L_h C}{2} \|x - y\|^2 \end{aligned}$$

and given  $y \neq x$ , we successively deduce that

$$\begin{aligned} f_z(x, \xi) - f_z(y, \xi) &= h(c(z, \xi) + \langle \nabla c(z, \xi), x - z \rangle) - h(c(z, \xi) + \langle \nabla c(z, \xi), y - z \rangle) \\ &\leq L_h |\langle \nabla c(z, \xi), x - y \rangle| \end{aligned} \tag{12}$$

$$\begin{aligned} &\leq L_h \frac{L_c \sqrt{2V_d(y, x)}}{\|x - y\|} \cdot \|x - y\| \\ &= L_h L_c \sqrt{2V_d(y, x)}, \end{aligned} \tag{13}$$

where (12) is by  $L_h$ -Lipschitzness of  $h$  and (13) is by Cauchy-Schwarz and the definition of  $L_c$ -relative Lipschitzness. The case  $x = y$  is straight-forward.

---

**Proof of Lemma 7**


---

Without loss of generality, we consider the following proximal mapping

$$\mathcal{A}(z, x, \xi) := \arg \min_w \{f_z(w, \xi) + \omega(w) + \gamma V_d(w, x)\},$$

where  $\mathcal{A}$  denotes the proximal mapping from two past iterates  $z, x$  and a given sample  $\xi' \sim \Xi$ . Then we invoke the three-point lemma to get, for any  $u \in \text{dom } d$  that

$$\begin{aligned} f_z(\mathcal{A}(z, x, \xi'), \xi') + \omega(\mathcal{A}(z, x, \xi')) + \gamma V_d(\mathcal{A}(z, x, \xi'), x) \\ \leq f_z(u, \xi') + \omega(u) + \gamma V_d(u, x) - \gamma V_d(u, \mathcal{A}(z, x, \xi')) \end{aligned} \quad (14)$$

Similarly, given some  $\xi \sim \Xi, v \in \text{dom } d$ , we have

$$\begin{aligned} f_z(\mathcal{A}(z, x, \xi), \xi) + \omega(\mathcal{A}(z, x, \xi)) + \gamma V_d(\mathcal{A}(z, x, \xi), x) \\ \leq f_z(v, \xi) + \omega(v) + \gamma V_d(v, x) - \gamma V_d(v, \mathcal{A}(z, x, \xi)). \end{aligned} \quad (15)$$

Letting  $u = \mathcal{A}(z, x, \xi)$  in (14) and  $v = \mathcal{A}(z, x, \xi')$  in (15), we sum the two relations up and get

$$\begin{aligned} & \gamma[V_d(\mathcal{A}(z, x, \xi'), \mathcal{A}(z, x, \xi)) + V_d(\mathcal{A}(z, x, \xi), \mathcal{A}(z, x, \xi'))] \\ & \leq f_z(\mathcal{A}(z, x, \xi), \xi') - f_z(\mathcal{A}(z, x, \xi'), \xi') + f_z(\mathcal{A}(z, x, \xi'), \xi) - f_z(\mathcal{A}(z, x, \xi), \xi) \\ & \leq L_f[\sqrt{2V_d(\mathcal{A}(z, x, \xi'), \mathcal{A}(z, x, \xi))} + \sqrt{2V_d(\mathcal{A}(z, x, \xi), \mathcal{A}(z, x, \xi'))}] \end{aligned} \quad (16)$$

$$\leq 2L_f[\sqrt{V_d(\mathcal{A}(z, x, \xi'), \mathcal{A}(z, x, \xi))} + \sqrt{V_d(\mathcal{A}(z, x, \xi), \mathcal{A}(z, x, \xi'))}] \quad (17)$$

where (16) is by Lipschitzness from **A2** and uses the relation  $\sqrt{a} + \sqrt{b} \leq \sqrt{2}\sqrt{a+b}$ . Then this implies

$$\begin{aligned} & \max \left\{ \sqrt{V_d(\mathcal{A}(z, x, \xi'), \mathcal{A}(z, x, \xi))}, \sqrt{V_d(\mathcal{A}(z, x, \xi), \mathcal{A}(z, x, \xi'))} \right\} \\ & \leq \sqrt{V_d(\mathcal{A}(z, x, \xi'), \mathcal{A}(z, x, \xi)) + V_d(\mathcal{A}(z, x, \xi), \mathcal{A}(z, x, \xi'))} \leq 2\gamma^{-1}L_f \leq \frac{2L_f}{\gamma - \kappa}. \end{aligned} \quad (18)$$

Last we successively deduce that

$$\begin{aligned} & |\mathbb{E}_{\xi'} \{ \mathbb{E}_{\xi} [f_z(\mathcal{A}(z, x, \xi'), \xi) - f_z(\mathcal{A}(z, x, \xi'), \xi')] \}| \\ & = \left| \int_{\xi' \sim \Xi} \int_{\xi \sim \Xi} f_z(\mathcal{A}(z, x, \xi'), \xi) - f_z(\mathcal{A}(z, x, \xi'), \xi') d\mu_{\xi} d\mu_{\xi'} \right| \\ & = \left| \int_{\xi' \sim \Xi} \int_{\xi \sim \Xi} f_z(\mathcal{A}(z, x, \xi'), \xi) d\mu_{\xi} d\mu_{\xi'} - \int_{\xi' \sim \Xi} f_z(\mathcal{A}(z, x, \xi'), \xi') d\mu_{\xi'} \right| \\ & = \left| \int_{\xi' \sim \Xi} \int_{\xi \sim \Xi} f_z(\mathcal{A}(z, x, \xi'), \xi) d\mu_{\xi} d\mu_{\xi'} - \int_{\xi \sim \Xi} f_z(\mathcal{A}(z, x, \xi), \xi) d\mu_{\xi} \right| \\ & = \left| \int_{\xi' \sim \Xi} \int_{\xi \sim \Xi} f_z(\mathcal{A}(z, x, \xi'), \xi) - f_z(\mathcal{A}(z, x, \xi), \xi) d\mu_{\xi} d\mu_{\xi'} \right| \\ & \leq \int_{\xi' \sim \Xi} \int_{\xi \sim \Xi} |f_z(\mathcal{A}(z, x, \xi'), \xi) - f_z(\mathcal{A}(z, x, \xi), \xi)| d\mu_{\xi} d\mu_{\xi'} \end{aligned} \quad (19)$$

$$\leq \int_{\xi' \sim \Xi} \int_{\xi \sim \Xi} L_f \cdot \max \left\{ \sqrt{V_d(\mathcal{A}(z, x, \xi), \mathcal{A}(z, x, \xi'))}, \sqrt{V_d(\mathcal{A}(z, x, \xi'), \mathcal{A}(z, x, \xi))} \right\} d\mu_{\xi} d\mu_{\xi'} \quad (20)$$

$$\leq \int_{\xi' \sim \Xi} \int_{\xi \sim \Xi} \frac{2L_f^2}{\gamma - \kappa} d\mu_{\xi} d\mu_{\xi'} = \frac{2L_f^2}{\gamma - \kappa}, \quad (21)$$

where the third equality holds since  $\xi$  and  $\xi'$  are from the same distribution; (19) follows from Jensen's inequality and the last inequality uses (18). Plugging in  $z = x^{k-\tau_k}$ ,  $x = x^k$ ,  $\xi' = \xi^{k-\tau_k}$  and  $\gamma = \gamma_k$  into (21) completes the proof.

---

### Proof of Lemma 8

---

First, we have, by the three-point lemma and optimality of  $\hat{x}^k$ , that

$$\begin{aligned} f_{x^{k-\tau_k}}(x^{k+1}, \xi^{k-\tau_k}) + \omega(x^{k+1}) + \gamma_k V_d(x^{k+1}, x^k) &\leq f_{x^{k-\tau_k}}(\hat{x}^k, \xi^{k-\tau_k}) + \omega(\hat{x}^k) + \gamma_k V_d(\hat{x}^k, x^k) - (\gamma_k - \kappa) V_d(\hat{x}^k, x^{k+1}) \\ f(\hat{x}^k) + \rho V_d(\hat{x}^k, x^k) &\leq f(x^{k+1}) + \rho V_d(x^{k+1}, x^k) \end{aligned}$$

Summing the above two relations and taking expectations, we have

$$\begin{aligned} &(\gamma_k - \rho) \mathbb{E}_k[V_d(x^{k+1}, x^k)] - (\gamma_k - \rho) V_d(\hat{x}^k, x^k) + (\gamma_k - \kappa) \mathbb{E}_k[V_d(\hat{x}^k, x^{k+1})] \\ &\leq f_{x^{k-\tau_k}}(\hat{x}^k, \xi^{k-\tau_k}) - f(\hat{x}^k) + \mathbb{E}_k[f(x^{k+1})] - \mathbb{E}_k[f_{x^{k-\tau_k}}(x^{k+1}, \xi^{k-\tau_k})] \\ &= f_{x^{k-\tau_k}}(\hat{x}^k, \xi^{k-\tau_k}) - f(\hat{x}^k) + \mathbb{E}_k[f(x^{k+1})] - \mathbb{E}_k[\mathbb{E}_\xi[f_{x^{k-\tau_k}}(x^{k+1}, \xi)]] \\ &\quad + \mathbb{E}_k[\mathbb{E}_\xi[f_{x^{k-\tau_k}}(x^{k+1}, \xi)]] - \mathbb{E}_k[f_{x^{k-\tau_k}}(x^{k+1}, \xi^{k-\tau_k})] \\ &\leq \frac{\lambda}{2} \|x^{k-\tau_k} - \hat{x}^k\|^2 + \frac{\lambda}{2} \mathbb{E}_k[\|x^{k+1} - x^{k-\tau_k}\|^2] + \frac{2L_f^2}{\gamma_k - \kappa}, \end{aligned} \tag{22}$$

where (22) uses **P2** and **Lemma 7**. Next we lower-bound the left-hand side using the 1-strong convexity of kernel  $d$

$$\begin{aligned} &\frac{\gamma_k - \rho}{2} \mathbb{E}_k[\|x^{k+1} - x^k\|^2] - (\gamma_k - \rho) V_d(\hat{x}^k, x^k) + (\gamma_k - \kappa) \mathbb{E}_k[V_d(\hat{x}^k, x^{k+1})] \\ &\leq (\gamma_k - \rho) \mathbb{E}_k[V_d(x^{k+1}, x^k)] - (\gamma_k - \rho) V_d(\hat{x}^k, x^k) + (\gamma_k - \kappa) \mathbb{E}_k[V_d(\hat{x}^k, x^{k+1})]. \end{aligned} \tag{23}$$

Re-arranging the terms,

$$(\gamma_k - \kappa) \mathbb{E}_k[V_d(\hat{x}^k, x^{k+1})] \tag{24}$$

$$\begin{aligned} &\leq (\gamma_k - \rho) V_d(\hat{x}^k, x^k) + \frac{\lambda}{2} \mathbb{E}_k[\|x^{k+1} - x^{k-\tau_k}\|^2] + \frac{\lambda}{2} \|x^{k-\tau_k} - \hat{x}^k\|^2 + \frac{2L_f^2}{\gamma_k - \kappa} \\ &\leq (\gamma_k - \rho) V_d(\hat{x}^k, x^k) + \frac{3\lambda}{2} \mathbb{E}_k[\|x^{k+1} - x^{k-\tau_k}\|^2] + \lambda \mathbb{E}_k[\|x^{k+1} - \hat{x}^k\|^2] + \frac{2L_f^2}{\gamma_k - \kappa} \end{aligned} \tag{25}$$

$$\begin{aligned} &= (\gamma_k - \rho) V_d(\hat{x}^k, x^k) + \frac{3\lambda}{2} \mathbb{E}_k[\|x^{k+1} - x^{k-\tau_k}\|^2] + \frac{2L_f^2}{\gamma_k - \kappa} + 2\lambda \mathbb{E}_k[V_d(\hat{x}^k, x^{k+1})] \\ &\quad + \lambda \mathbb{E}_k[\|x^{k+1} - \hat{x}^k\|^2 - 2V_d(\hat{x}^k, x^{k+1})] \\ &\leq (\gamma_k - \rho) V_d(\hat{x}^k, x^k) + \frac{3\lambda}{2} \mathbb{E}_k[\|x^{k+1} - x^{k-\tau_k}\|^2] + \frac{2L_f^2}{\gamma_k - \kappa} + 2\lambda \mathbb{E}_k[V_d(\hat{x}^k, x^{k+1})] \end{aligned} \tag{26}$$

where the (25) uses  $\|a + b\|^2 \leq 2\|a\|^2 + 2\|b\|^2$  and (26) again follows by  $V_d(\hat{x}^k, x^{k+1}) \geq \frac{1}{2} \|x^{k+1} - \hat{x}^k\|^2$ . Now we re-arrange the terms and divide both sides by  $\gamma_k - 2\lambda - \kappa$  to get

$$\begin{aligned} &\mathbb{E}_k[V_d(\hat{x}^k, x^{k+1})] \\ &\leq \frac{\gamma_k - \rho}{\gamma_k - 2\lambda - \kappa} V_d(\hat{x}^k, x^k) + \frac{2L_f^2}{\gamma_k(\gamma_k - 2\lambda - \kappa)} + \frac{3\lambda}{2(\gamma_k - 2\lambda - \kappa)} \mathbb{E}_k[\|x^{k+1} - x^{k-\tau_k}\|^2] \\ &= V_d(\hat{x}^k, x^k) - \frac{\rho - 2\lambda - \kappa}{\gamma_k - 2\lambda - \kappa} V_d(\hat{x}^k, x^k) + \frac{2L_f^2}{\gamma_k(\gamma_k - 2\lambda - \kappa)} + \frac{3\lambda}{2(\gamma_k - 2\lambda - \kappa)} \mathbb{E}_k[\|x^{k+1} - x^{k-\tau_k}\|^2] \end{aligned} \tag{27}$$

Now we are ready to evaluate the decrease in the potential function.

$$\begin{aligned}
& \mathbb{E}_k[\psi_{1/\rho}^d(x^{k+1})] \\
&= \mathbb{E}_k[f(\hat{x}^{k+1}) + \omega(\hat{x}^{k+1}) + \rho V_d(\hat{x}^{k+1}, x^{k+1})] \\
&\leq \mathbb{E}_k[f(\hat{x}^k) + \omega(\hat{x}^k) + \rho V_d(\hat{x}^k, x^{k+1})] \\
&\leq f(\hat{x}^k) + \omega(\hat{x}^k) + \rho V_d(\hat{x}^k, x^k) - \frac{\rho(\rho - 2\lambda - \kappa)}{\gamma_k - 2\lambda - \kappa} V_d(\hat{x}^k, x^k) \\
&\quad + \frac{3\rho\lambda}{2(\gamma_k - 2\lambda - \kappa)} \mathbb{E}_k[\|x^{k+1} - x^{k-\tau_k}\|^2] + \frac{2\rho L_f^2}{\gamma_k(\gamma_k - 2\lambda - \kappa)} \\
&= \psi_{1/\rho}^d(x^k) - \frac{\rho(\rho - 2\lambda - \kappa)}{\gamma_k - 2\lambda - \kappa} V_d(\hat{x}^k, x^k) \\
&\quad + \frac{3\rho\lambda}{2(\gamma_k - 2\lambda - \kappa)} \mathbb{E}_k[\|x^{k+1} - x^{k-\tau_k}\|^2] + \frac{2\rho L_f^2}{\gamma_k(\gamma_k - 2\lambda - \kappa)},
\end{aligned} \tag{28}$$

where (28) plugs in the relation from (27). Another re-arrangement completes the proof.

---

### Proof of Theorem 5

---

Summing the relation from **Lemma 8** from  $k = 1, \dots, K$ ,

$$\begin{aligned}
& \rho(\rho - 2\lambda - \kappa) \mathbb{E}[V_d(\hat{x}^{k^*}, x^{k^*})] \\
&= \frac{\rho(\rho - 2\lambda - \kappa)}{K} \sum_{k=1}^K V_d(\hat{x}^k, x^k) \\
&\leq \frac{\gamma - 2\lambda - \kappa}{K} \{\psi_{1/\rho}^d(x^1) - \mathbb{E}_k[\psi_{1/\rho}^d(x^{K+1})]\} + \frac{2\rho L_f^2}{\gamma - \kappa} + \frac{3\rho\lambda}{2K} \sum_{k=1}^K \mathbb{E}_k[\|x^{k+1} - x^{k-\tau_k}\|^2]. \\
&\leq \frac{(\gamma - 2\lambda - \kappa)D}{K} + \frac{2\rho L_f^2}{\gamma - \kappa} + \frac{3\rho\lambda}{2K} \sum_{k=1}^K \mathbb{E}_k[\|x^{k+1} - x^{k-\tau_k}\|^2].
\end{aligned} \tag{29}$$

Now it remains to bound the error from the stochastic delays and we invoke **Lemma 6** to successively deduce that

$$\begin{aligned}
\sum_{k=1}^K \mathbb{E}_k[\|x^{k+1} - x^{k-\tau_k}\|^2] &= \sum_{k=1}^K \sum_{j=0}^{\infty} p_j \mathbb{E}_k[\|x^{k+1} - x^{k-j}\|^2] \\
&= \sum_{k=1}^K \sum_{j=0}^{\infty} p_j \mathbb{E}_k \left[ \left\| \sum_{l=0}^j x^{k+1-l} - x^{k-l} \right\|^2 \right] \\
&\leq \sum_{k=1}^K \sum_{j=0}^{\infty} p_j \mathbb{E}_k \left[ \sum_{l=0}^j \|x^{k+1-l} - x^{k-l}\|^2 \right]
\end{aligned} \tag{30}$$

$$\leq 2K \left( \frac{L_f + L_\omega}{\gamma} \right)^2 \sum_{k=1}^K \sum_{j=0}^{\infty} p_j (j+1)^2 \tag{31}$$

$$= 2K \left( \frac{L_f + L_\omega}{\gamma} \right)^2 (\tau_{\sigma^2} + 2\bar{\tau} + 1), \tag{32}$$

and we have

$$\begin{aligned}\rho(\rho - 2\lambda - \kappa)\mathbb{E}[V_d(\hat{x}^{k^*}, x^{k^*})] &\leq \frac{(\gamma - 2\lambda - \kappa)D}{K} + \frac{2\rho L_f^2}{\gamma - \kappa} + 3\rho\lambda \left(\frac{L_f + L_\omega}{\gamma}\right)^2 (\tau_{\sigma^2} + 2\bar{\tau} + 1). \\ &\leq \frac{D}{\sqrt{K}\alpha} + \frac{2\rho L_f^2\alpha}{\sqrt{K}} + \frac{3\rho\lambda(L_f + L_\omega)^2\alpha^2}{K}(\tau_{\sigma^2} + 2\bar{\tau} + 1)\end{aligned}\quad (33)$$

Dividing both sides of (33) by  $\rho(\rho - 2\lambda - \kappa)$  completes the proof.

## B.4 Proof of Main Results in Section 3

First  $d(x) = \frac{1}{2}\|x\|^2$  satisfies **A4'**. Since **A1**, **A2**, **A3**, **A4** and **B1** are equivalent to **A1'**, **A2'**, **A3'**, **A5'** and **B1'**, we complete the proof.

## B.5 Kernel and Subproblems

In this section, we discuss the practical aspects for the Bregman proximal methods. More specifically we discuss how to construct proper divergence kernels for DSPL so that we can accommodate *polynomial growth* in the objective. We also propose subroutines to solve the Bregman proximal subproblems efficiently for a wide class of common loss functions in machine learning tasks.

### B.5.1 Choosing the Divergence Kernel

The first ingredient of the Bregman proximal method is the choice of the kernel function. The choice of kernel has been broadly discussed in literature [11, 25] and we borrow the results therein to construct proper kernels for both DSMD and DSPL. Also, due to the assumptions we made throughout the paper, it suffices to consider kernels  $d(x) = \mathcal{P}_n^p(\|x\|) := \sum_{k=0}^n p_k \|x\|^k$  that are degree- $n$  polynomials in  $\|x\|$ . First, we recall the following lemma and refer the readers to [25] for its proof.

**Lemma 9.** *Given  $h(x)$  such that  $\|h'(x)\|^2 \leq \mathcal{P}_n^p(\|x\|) = \sum_{k=0}^n p_k \|x\|^k, p \geq 0, \forall x \in \text{dom } h$ ,  $h$  is 1-Lipschitz continuous relative to  $d(x) := \sum_{k=0}^n \frac{p_k}{k+2} \|x\|^{k+2}$ .*

The lemma implies that once we establish a polynomial upper bound on the subgradient norm of  $\omega$ , a kernel  $h$  is immediately available. Recall that in DSPL, we have  $f(x, \xi) = h(c(x, \xi))$  and allow relative continuity in both  $c$  and  $\omega$ . To build a kernel for  $f(x, \xi) + \omega(x)$ , we simply invoke **Lemma 9** twice, get two kernels  $d_c(x)$  and  $d_\omega(x)$  and adopt  $d_c(x) + d_\omega(x)$  as the kernel we need.

*Remark 13.* We note that the above kernel covers most applications [10] of prox-linear method including phase retrieval, blind deconvolution, matrix completion, covariance estimation, robust PCA, and so forth. Since in most machine learning applications,  $c$  is a quadratic function,  $\nabla c$  is bounded by first-order growth.

Now that we have specified ways to construct kernels for DSPL, in the next section we discuss how to solve the Bregman proximal subproblems. The solution of the subproblems determines the practical applicability of our methods, and we show that these subproblems can be efficiently solved for a wide range of problems.

### B.5.2 Bregman Proximal Subproblem

In this section, we discuss the solution of the proximal subproblems for DSPL when  $\omega = 0$ , where the Bregman proximal subproblem can then be summarized as

$$\min_x h(\langle a, x \rangle + b) + V_d(x, y). \quad (34)$$

And we consider piece-wise linear  $h(x) = \max\{\alpha_1 x + \beta_1, \alpha_2 x + \beta_2\}$ . This formulation characterizes common nonsmooth loss functions including  $\ell_1$  loss  $|x| = \max\{x, -x\}$  and hinge loss  $\max\{0, x\}$ . Substituting  $h$  in and

removing terms irrelevant to  $x$ , we arrive at the following DSPL subproblem.

$$\min_x \max\{\langle a_1, x \rangle + b_1, \langle a_2, x \rangle + b_2\} + d(x) \quad (35)$$

The next proposition provides a solution to the above subproblem.

**Proposition 3** (Solving the proximal subproblem). *The proximal subproblem can be solved by evaluating solutions to the following three problems*

$$\begin{aligned} \min_x \langle a_1, x \rangle + d(x) \\ \min_x \langle a_2, x \rangle + d(x), \end{aligned}$$

and

$$\begin{aligned} \min_x \quad & \langle a_1, x \rangle + d(x) \\ \text{subject to} \quad & \langle a_1 - a_2, x \rangle + b_1 - b_2 = 0, \end{aligned}$$

where the solution to the third problem satisfies  $x = u + \alpha v$ , where  $u = -\frac{(a_1 - a_2)(b_1 - b_2)}{\|a_1 - a_2\|^2}$ ,  $v = \frac{(\|a_1\|^2 - \|a_2\|^2)}{2\|a_1 - a_2\|^2}(a_1 - a_2) - \frac{a_1 + a_2}{2}$  and  $\alpha$  is a positive root of the following equation

$$\sum_{k=0}^n p_k \alpha \|u + \alpha v\|^{k+1} - 1 = 0.$$

*Proof.* Recall that we are solving the following convex optimization problem

$$\min_x \max\{\langle a_1, x \rangle + b_1, \langle a_2, x \rangle + b_2\} + d(x),$$

where  $d$  is strongly convex and thus the problem admits a unique minimizer  $x^*$ . Then we do case analysis.

**Case 1.**  $\langle a_1, x^* \rangle + b_1 > \langle a_2, x^* \rangle + b_2$ . In this case solving  $\min_x \langle a_1, x \rangle + d(x)$  produces  $x^*$ .

**Case 2.**  $\langle a_1, x^* \rangle + b_1 < \langle a_2, x^* \rangle + b_2$ . In this case solving  $\min_x \langle a_2, x \rangle + d(x)$  produces  $x^*$ .

The above two cases degenerate into the subproblems from stochastic mirror descent and its solution has been discussed in [25]. The last case is a bit more tricky.

**Case 3.**  $\langle a_1, x^* \rangle + b_1 = \langle a_2, x^* \rangle + b_2$ .

In this case, the proximal subproblem becomes an equality constrained problem.

$$\begin{aligned} \min_x \quad & \langle a_1, x \rangle + d(x) \\ \text{subject to} \quad & \langle a_1 - a_2, x \rangle + b_1 - b_2 = 0 \end{aligned}$$

Letting  $\lambda$  be the multiplier of the equality constraint and appealing to the optimality condition, we have

$$a_1 + \nabla d(x) + \lambda(a_1 - a_2) = 0 \quad (36)$$

$$a_2 + \nabla d(x) + \lambda(a_1 - a_2) = 0 \quad (37)$$

$$\langle a_1 - a_2, x \rangle + b_1 - b_2 = 0. \quad (38)$$

Summing (36) (37) and dividing both sides by 2, we have

$$\frac{a_1 + a_2}{2} + \nabla d(x) + \lambda(a_1 - a_2) = 0. \quad (39)$$



Multiplying both sides of (39) by  $a_1 - a_2$ , we arrive at

$$\frac{\|a_1\|^2 - \|a_2\|^2}{2} + \langle a_1 - a_2, \nabla d(x) \rangle + \lambda \|a_1 - a_2\|^2 = 0. \quad (40)$$

Since  $d(x)$  is a polynomial in  $\|x\|$ ,  $\nabla d(x) = \zeta x$ ,  $\zeta > 0$  and using (38), we have

$$\lambda = \frac{b_1 - b_2}{\|a_1 - a_2\|^2} \zeta - \frac{\|a_1\|^2 - \|a_2\|^2}{2\|a_1 - a_2\|^2}. \quad (41)$$

Then substituting  $\lambda$  into (40),

$$\begin{aligned} 0 &= \frac{a_1 + a_2}{2} + \nabla d(x) + \lambda(a_1 - a_2) \\ &= \frac{a_1 + a_2}{2} + \zeta x + \zeta \frac{(a_1 - a_2)(b_1 - b_2)}{\|a_1 - a_2\|^2} - \frac{\|a_1\|^2 - \|a_2\|^2}{2\|a_1 - a_2\|^2} (a_1 - a_2) \\ &= \zeta \left[ x + \frac{(a_1 - a_2)(b_1 - b_2)}{\|a_1 - a_2\|^2} \right] - \frac{\|a_1\|^2 - \|a_2\|^2}{2\|a_1 - a_2\|^2} (a_1 - a_2) + \frac{a_1 + a_2}{2} \end{aligned}$$

we get

$$x = \zeta^{-1} \left[ \frac{(\|a_1\|^2 - \|a_2\|^2)}{2\|a_1 - a_2\|^2} (a_1 - a_2) - \frac{a_1 + a_2}{2} \right] - \frac{(a_1 - a_2)(b_1 - b_2)}{\|a_1 - a_2\|^2}$$

for some  $\zeta > 0$ . Without loss of generality we express  $x = u + \alpha v$  for  $u = -\frac{(a_1 - a_2)(b_1 - b_2)}{\|a_1 - a_2\|^2}$  and  $v = \frac{(\|a_1\|^2 - \|a_2\|^2)}{2\|a_1 - a_2\|^2} (a_1 - a_2) - \frac{a_1 + a_2}{2}$  and  $\alpha > 0$ . Substituting back gives  $\zeta = \sum_{k=0}^n p_k \|x\|^{k+1}$  and

$$\begin{aligned} \|\zeta(x - u) - v\| &= \|\alpha \zeta v - v\| \\ &= |\alpha \zeta - 1| \cdot \|v\| \\ &= 0. \end{aligned}$$

and we only need to verify the positive roots of  $\sum_{k=0}^n p_k \alpha \|u + \alpha v\|^{k+1} - 1 = 0$ , which can be efficiently solved if  $n$  is not large. This completes the proof.  $\square$

## C Convergence Analysis of DSEPL

In this section we present the convergence analysis for DSEPL.

### C.1 Auxiliary Results

To show the convergence of DSEPL, we need to define an auxiliary sequence

$$z^k := x^k + \frac{\beta}{1 - \beta} (x^k - x^{k-1}).$$

Given  $x^k$ , define  $\bar{x} = \beta x^k + (1 - \beta)x$  for  $x \in \text{dom}(\omega)$  and  $\theta = 1 - \beta$ . Then the following identities hold

$$\begin{aligned} \bar{x} - x^k &= \theta(x - x^k) \\ \bar{x} - y^k &= \theta(x - z^k) \\ \bar{x} - x^{k+1} &= \theta(x - z^{k+1}). \end{aligned}$$

and will be used frequently in the analysis.

## C.2 Proof of Lemma 2

First by the  $(\gamma - \kappa)$ -strong convexity of the proximal sub-problem, we have

$$\begin{aligned}
& f_{x^{k-\tau_k}}(x^{k+1}, \xi^{k-\tau_k}) + \omega(x^{k+1}) + \frac{\gamma}{2} \|x^{k+1} - y^k\|^2 \\
& \leq f_{x^{k-\tau_k}}(\bar{x}, \xi^{k-\tau_k}) + \omega(\bar{x}) + \frac{\gamma}{2} \|\bar{x} - y^k\|^2 - \frac{\gamma - \kappa}{2} \|x^{k+1} - \bar{x}\|^2 \\
& = f_{x^{k-\tau_k}}(\bar{x}, \xi^{k-\tau_k}) + \omega(\bar{x}) + \frac{\gamma\theta^2}{2} \|x - z^k\|^2 - \frac{(\gamma - \kappa)\theta^2}{2} \|x - z^{k+1}\|^2.
\end{aligned} \tag{42}$$

Also, since  $f_{x^{k-\tau_k}}(\cdot, \xi^{k-\tau_k}) + \omega(\cdot) + \frac{\kappa}{2} \|\cdot - x^k\|^2$  is convex, we plug  $\bar{x}$  in and apply convexity to get that

$$\begin{aligned}
& f_{x^{k-\tau_k}}(\bar{x}, \xi^{k-\tau_k}) + \omega(\bar{x}) + \frac{\kappa}{2} \|\bar{x} - x^k\|^2 \\
& \leq (1 - \theta) [f_{x^{k-\tau_k}}(x^k, \xi^{k-\tau_k}) + \omega(x^k)] + \theta \left[ f_{x^{k-\tau_k}}(x, \xi^{k-\tau_k}) + \omega(x) + \frac{\kappa}{2} \|x - x^k\|^2 \right] \\
& \leq (1 - \theta) [f_{x^{k-\tau_k}}(x^k, \xi^{k-\tau_k}) + \omega(x^k)] + \theta \left[ f(x) + \omega(x) + \frac{\kappa}{2} \|x - x^k\|^2 + \frac{\lambda}{2} \|x - x^{k-\tau_k}\|^2 \right],
\end{aligned}$$

where the second inequality leverages two-sided approximation since  $|f_{x^{k-\tau_k}}(x, \xi^{k-\tau_k}) - f(x)| \leq \frac{\lambda}{2} \|x - x^{k-\tau_k}\|^2$ . Then a simple re-arrangement gives

$$\begin{aligned}
& f_{x^{k-\tau_k}}(\bar{x}, \xi^{k-\tau_k}) + \omega(\bar{x}) \\
& \leq (1 - \theta) [f_{x^{k-\tau_k}}(x^k, \xi^{k-\tau_k}) + \omega(x^k)] \\
& \quad + \theta \left[ f(x) + \omega(x) + \frac{\kappa}{2} \|x - x^k\|^2 + \frac{\lambda}{2} \|x - x^{k-\tau_k}\|^2 \right] - \frac{\kappa\theta^2}{2} \|x - x^k\|^2.
\end{aligned}$$

Now combining the above inequality with (42), we get that

$$\begin{aligned}
& f_{x^{k-\tau_k}}(x^{k+1}, \xi^{k-\tau_k}) + \omega(x^{k+1}) + \frac{\gamma}{2} \|x^{k+1} - y^k\|^2 \\
& \leq (1 - \theta) [f_{x^{k-\tau_k}}(x^k, \xi^{k-\tau_k}) + \omega(x^k)] + \theta \left[ f(x) + \omega(x) + \frac{\kappa}{2} \|x - x^k\|^2 + \frac{\lambda}{2} \|x - x^{k-\tau_k}\|^2 \right] \\
& \quad - \frac{\kappa\theta^2}{2} \|x - x^k\|^2 + \frac{\gamma\theta^2}{2} \|x - z^k\|^2 - \frac{(\gamma - \kappa)\theta^2}{2} \|x - z^{k+1}\|^2.
\end{aligned} \tag{43}$$

From now on we let  $x = \hat{z}^k$  in (43) and successively deduce that

$$\begin{aligned}
& f_{x^{k-\tau_k}}(x^{k+1}, \xi^{k-\tau_k}) + \omega(x^{k+1}) + \frac{\gamma}{2} \|x^{k+1} - y^k\|^2 \\
& \leq (1 - \theta) [f_{x^{k-\tau_k}}(x^k, \xi^{k-\tau_k}) + \omega(x^k)] + \theta \left[ f(\hat{z}^k) + \omega(\hat{z}^k) + \frac{\kappa}{2} \|\hat{z}^k - x^k\|^2 + \frac{\lambda}{2} \|\hat{z}^k - x^{k-\tau_k}\|^2 \right] \\
& \quad - \frac{\kappa\theta^2}{2} \|\hat{z}^k - x^k\|^2 + \frac{\gamma\theta^2}{2} \|\hat{z}^k - z^k\|^2 - \frac{(\gamma - \kappa)\theta^2}{2} \|\hat{z}^k - z^{k+1}\|^2 \\
& = (1 - \theta) [f_{x^{k-\tau_k}}(x^k, \xi^{k-\tau_k}) + \omega(x^k)] + \theta [f(\hat{z}^k) + \omega(\hat{z}^k)] + \frac{\kappa\theta - \kappa\theta^2}{2} \|\hat{z}^k - x^k\|^2 + \frac{\lambda\theta}{2} \|\hat{z}^k - x^{k-\tau_k}\|^2 \\
& \quad + \frac{\gamma\theta^2}{2} \|\hat{z}^k - z^k\|^2 - \frac{(\gamma - \kappa)\theta^2}{2} \|\hat{z}^k - z^{k+1}\|^2 \\
& \leq (1 - \theta) [f_{x^{k-\tau_k}}(x^k, \xi^{k-\tau_k}) + \omega(x^k)] + \theta [f(\hat{z}^k) + \omega(\hat{z}^k)] + \frac{\lambda\theta}{2} \|\hat{z}^k - x^{k-\tau_k}\|^2 \\
& \quad + \frac{\gamma\theta^2}{2} \|\hat{z}^k - z^k\|^2 - \frac{(\gamma - \kappa)\theta^2}{2} \|\hat{z}^k - z^{k+1}\|^2 + \theta\kappa\beta [\|x^{k+1} - x^k\|^2 + \|\hat{z}^k - x^{k+1}\|^2]
\end{aligned} \tag{44}$$

$$\begin{aligned}
& \leq (1 - \theta) [f_{x^{k-\tau_k}}(x^k, \xi^{k-\tau_k}) + \omega(x^k)] + \theta [f(\hat{z}^k) + \omega(\hat{z}^k)] + \theta(\kappa\beta + \lambda) \|\hat{z}^k - x^{k+1}\|^2 \\
& \quad + \lambda\theta \|x^{k+1} - x^{k-\tau_k}\|^2 + \frac{\gamma\theta^2}{2} \|\hat{z}^k - z^k\|^2 - \frac{(\gamma - \kappa)\theta^2}{2} \|\hat{z}^k - z^{k+1}\|^2 + \theta\kappa\beta \|x^{k+1} - x^k\|^2,
\end{aligned} \tag{45}$$

where the second inequality (44) applies  $\|\hat{z}^k - x^k\|^2 \leq 2[\|x^{k+1} - x^k\|^2 + \|\hat{z}^k - x^{k+1}\|^2]$  and the last inequality applies  $\|\hat{z}^k - x^{k-\tau_k}\|^2 \leq 2\|\hat{z}^k - x^{k+1}\|^2 + 2\|x^{k+1} - x^{k-\tau_k}\|^2$ .

By definition of  $\hat{z}^k$ , for  $\rho > \lambda + \kappa$ , we have  $(\rho - \lambda - \kappa)$ -strong convexity of  $\psi(x) + \frac{\rho}{2}\|\cdot - x\|^2$  and

$$\begin{aligned} & f(\hat{z}^k) + \omega(\hat{z}^k) + \frac{\rho}{2}\|\hat{z}^k - z^k\|^2 \\ & \leq f(x^{k+1}) + \omega(x^{k+1}) + \frac{\rho}{2}\|x^{k+1} - z^k\|^2 - \frac{\rho - \lambda - \kappa}{2}\|x^{k+1} - \hat{z}^k\|^2. \end{aligned} \quad (46)$$

Multiplying (46) by  $\theta$  and adding it to (45), we have

$$\begin{aligned} & \frac{\gamma}{2}\|x^{k+1} - y^k\|^2 \\ & \leq (1 - \theta) [f_{x^{k-\tau_k}}(x^k, \xi^{k-\tau_k}) + \omega(x^k)] + \theta f(x^{k+1}) - f_{x^{k-\tau_k}}(x^{k+1}, \xi^{k-\tau_k}) - (1 - \theta)\omega(x^{k+1}) \\ & \quad + \frac{\rho\theta}{2}\|x^{k+1} - z^k\|^2 - \frac{\theta(\rho - 3\lambda - 2\kappa\beta - \kappa)}{2}\|x^{k+1} - \hat{z}^k\|^2 + \lambda\theta\|x^{k+1} - x^{k-\tau_k}\|^2 \\ & \quad + \frac{\gamma\theta^2 - \rho\theta}{2}\|\hat{z}^k - z^k\|^2 - \frac{(\gamma - \kappa)\theta^2}{2}\|\hat{z}^k - z^{k+1}\|^2 + \theta\kappa\beta\|x^{k+1} - x^k\|^2. \end{aligned} \quad (47)$$

Then we bound the first line of the right hand side in (47) by

$$\begin{aligned} & (1 - \theta) [f_{x^{k-\tau_k}}(x^k, \xi^{k-\tau_k}) + \omega(x^k)] + \theta f(x^{k+1}) - f_{x^{k-\tau_k}}(x^{k+1}, \xi^{k-\tau_k}) - (1 - \theta)\omega(x^{k+1}) \\ & \leq (1 - \theta)[f(x^k, \xi^{k-\tau_k}) + \omega(x^k) - f(x^{k+1}) - \omega(x^{k+1})] + f(x^{k+1}) - \mathbb{E}_\xi [f_{x^{k-\tau_k}}(x^{k+1}, \xi)] \\ & \quad + \mathbb{E}_\xi [f_{x^{k-\tau_k}}(x^{k+1}, \xi)] - f_{x^{k-\tau_k}}(x^{k+1}, \xi^{k-\tau_k}) + \frac{(1 - \theta)\lambda}{2}\|x^k - x^{k-\tau_k}\|^2 \\ & \leq (1 - \theta)[f(x^k, \xi^{k-\tau_k}) + \omega(x^k) - f(x^{k+1}) - \omega(x^{k+1})] + \frac{2L_f^2}{\gamma - \kappa} \\ & \quad + \frac{\lambda}{2}[\|x^{k+1} - x^{k-\tau_k}\|^2 + (1 - \theta)\|x^k - x^{k-\tau_k}\|^2], \end{aligned} \quad (48)$$

where the inequalities invoke two-sided approximation  $|f_{x^{k-\tau_k}}(x^k, \xi^{k-\tau_k}) - f(x^k, \xi^{k-\tau_k})| \leq \frac{\lambda}{2}\|x^k - x^{k-\tau_k}\|^2$  and bound  $\mathbb{E}_\xi [f_{x^{k-\tau_k}}(x^{k+1}, \xi)] - f_{x^{k-\tau_k}}(x^{k+1}, \xi^{k-\tau_k})$  with **Lemma 7**. Now plugging (48) back into (47) gives

$$\begin{aligned} & \frac{\gamma}{2}\|x^{k+1} - y^k\|^2 \\ & \leq (1 - \theta)[f(x^k, \xi^{k-\tau_k}) + \omega(x^k) - f(x^{k+1}) - \omega(x^{k+1})] + \frac{2L_f^2}{\gamma - \kappa} \\ & \quad + \frac{\rho\theta}{2}\|x^{k+1} - z^k\|^2 - \frac{\theta(\rho - 3\lambda - 2\kappa\beta - \kappa)}{2}\|x^{k+1} - \hat{z}^k\|^2 \\ & \quad + \frac{\gamma\theta^2 - \rho\theta}{2}\|\hat{z}^k - z^k\|^2 - \frac{(\gamma - \kappa)\theta^2}{2}\|\hat{z}^k - z^{k+1}\|^2 + \theta\kappa\beta\|x^{k+1} - x^k\|^2 \\ & \quad + \left(\lambda\theta + \frac{\lambda}{2}\right)\|x^{k+1} - x^{k-\tau_k}\|^2 + \frac{\lambda(1 - \theta)}{2}\|x^k - x^{k-\tau_k}\|^2. \end{aligned} \quad (49)$$

Isolating the delayed error by  $\varepsilon_k = (\lambda\theta + \frac{\lambda}{2})\|x^{k+1} - x^{k-\tau_k}\|^2 + \frac{\lambda(1 - \theta)}{2}\|x^k - x^{k-\tau_k}\|^2$  and we have, by algebraic manipulations of the momentum terms, that

$$\begin{aligned} \|x^{k+1} - y^k\|^2 & = \|x^{k+1} - x^k + x^k - y^k\|^2 \\ & \geq \|x^{k+1} - x^k\|^2 + \beta^2\|x^k - x^{k-1}\|^2 - \beta\|x^{k+1} - x^k\|^2 - \beta\|x^k - x^{k-1}\|^2 \\ & = \theta\|x^{k+1} - x^k\|^2 - \beta\theta\|x^k - x^{k-1}\|^2 \end{aligned} \quad (50)$$

and that

$$\frac{\rho\theta}{2}\|x^{k+1} - z^k\|^2 \leq \rho\theta\|x^{k+1} - x^k\|^2 + \rho\beta^2\theta^{-1}\|x^k - x^{k-1}\|^2. \quad (51)$$

Combining (50), (51) with (49) and taking expectation, we have

$$\begin{aligned} & \frac{\gamma\theta}{2}\mathbb{E}_k[\|x^{k+1} - x^k\|^2] - \frac{\gamma\beta\theta}{2}\|x^k - x^{k-1}\|^2 \\ & \leq (1-\theta)\{\psi(x^k) - \mathbb{E}_k[\psi(x^{k+1})]\} + \frac{2L_f^2}{\gamma - \kappa} \\ & \quad + (\rho + \kappa\beta)\theta\mathbb{E}_k[\|x^{k+1} - x^k\|^2] + \rho\beta^2\theta^{-1}\|x^k - x^{k-1}\|^2 - \frac{\theta(\rho - 3\lambda - 2\kappa\beta - \kappa)}{2}\mathbb{E}_k[\|x^{k+1} - \hat{z}^k\|^2] \\ & \quad + \frac{\gamma\theta^2 - \rho\theta}{2}\|\hat{z}^k - z^k\|^2 - \frac{(\gamma - \kappa)\theta^2}{2}\mathbb{E}_k[\|\hat{z}^k - z^{k+1}\|^2] + \mathbb{E}_k[\varepsilon_k]. \end{aligned}$$

After re-arrangement, we arrive at

$$\begin{aligned} & \frac{(\gamma - \kappa)\theta^2}{2}\mathbb{E}_k[\|\hat{z}^k - z^{k+1}\|^2] \\ & \leq (1-\theta)\{\psi(x^k) - \mathbb{E}_k[\psi(x^{k+1})]\} + \frac{\gamma\theta^2 - \rho\theta}{2}\|\hat{z}^k - z^k\|^2 \\ & \quad + \left(\rho\beta^2\theta^{-1} + \frac{\gamma\beta\theta}{2}\right)\{\|x^k - x^{k-1}\|^2 - \mathbb{E}_k[\|x^{k+1} - x^k\|^2]\} - \frac{\theta(\rho - 3\lambda - 2\kappa\beta - \kappa)}{2}\mathbb{E}_k[\|x^{k+1} - \hat{z}^k\|^2] \\ & \quad + \frac{2L_f^2}{\gamma - \kappa} - \frac{\gamma\theta^2 - 2\theta(\rho + \kappa\beta) - 2\rho\beta^2\theta^{-1}}{2}\mathbb{E}_k[\|x^{k+1} - x^k\|^2] + \mathbb{E}_k[\varepsilon_k]. \end{aligned} \quad (52)$$

Dividing both sides of (52) by  $\frac{(\gamma - \kappa)\theta^2}{2}$ , we obtain that

$$\begin{aligned} & \mathbb{E}_k[\|\hat{z}^k - z^{k+1}\|^2] \\ & \leq \frac{2(1-\theta)}{(\gamma - \kappa)\theta^2}\{\psi(x^k) - \mathbb{E}_k[\psi(x^{k+1})]\} + \frac{\gamma\theta - \rho}{(\gamma - \kappa)\theta}\|\hat{z}^k - z^k\|^2 \\ & \quad + \frac{2\rho\beta^2\theta^{-1} + \gamma\beta\theta}{(\gamma - \kappa)\theta^2}\{\|x^k - x^{k-1}\|^2 - \mathbb{E}_k[\|x^{k+1} - x^k\|^2]\} - \frac{\rho - 3\lambda - 2\kappa\beta - \kappa}{(\gamma - \kappa)\theta}\mathbb{E}_k[\|x^{k+1} - \hat{z}^k\|^2] \\ & \quad + \frac{4L_f^2}{(\gamma - \kappa)^2\theta^2} - \frac{\gamma\theta^2 - 2\theta(\rho + \kappa\beta) - 2\rho\beta^2\theta^{-1}}{(\gamma - \kappa)\theta^2}\mathbb{E}_k[\|x^{k+1} - x^k\|^2] + \frac{2\mathbb{E}_k[\varepsilon_k]}{(\gamma - \kappa)\theta^2} \\ & = \|\hat{z}^k - z^k\|^2 - \frac{\rho - \kappa\theta}{(\gamma - \kappa)\theta}\|\hat{z}^k - z^k\|^2 + \frac{2\beta}{(\gamma - \kappa)\theta}\{\psi(x^k) - \mathbb{E}_k[\psi(x^{k+1})]\} \\ & \quad + \frac{2\rho\beta^2\theta^{-1} + \gamma\beta\theta}{(\gamma - \kappa)\theta^2}\{\|x^k - x^{k-1}\|^2 - \mathbb{E}_k[\|x^{k+1} - x^k\|^2]\} - \frac{\rho - 3\lambda - 2\kappa\beta - \kappa}{(\gamma - \kappa)\theta}\mathbb{E}_k[\|x^{k+1} - \hat{z}^k\|^2] \\ & \quad + \frac{4L_f^2}{(\gamma - \kappa)^2\theta^2} - \frac{\gamma\theta^2 - 2\theta(\rho + \kappa\beta) - 2\rho\beta^2\theta^{-1}}{(\gamma - \kappa)\theta^2}\mathbb{E}_k[\|x^{k+1} - x^k\|^2] + \frac{2\mathbb{E}_k[\varepsilon_k]}{(\gamma - \kappa)\theta^2}. \end{aligned} \quad (53)$$

Next, we consider the Moreau envelop and

$$\begin{aligned}
& \mathbb{E}_k[\psi_{1/\rho}(z^{k+1})] \\
&= \mathbb{E}_k \left[ \psi(\hat{z}^{k+1}) + \frac{\rho}{2} \|\hat{z}^{k+1} - z^{k+1}\|^2 \right] \\
&\leq \mathbb{E}_k \left[ f(\hat{z}^k) + \omega(\hat{z}^k) + \frac{\rho}{2} \|\hat{z}^k - z^{k+1}\|^2 \right] \\
&\leq f(\hat{z}^k) + \omega(\hat{z}^k) + \frac{\rho}{2} \|\hat{z}^k - z^k\|^2 + \frac{\rho\beta}{(\gamma - \kappa)\theta^2} \{\psi(x^k) - \mathbb{E}_k[\psi(x^{k+1})]\} \\
&\quad - \frac{\rho(\rho - \kappa\theta)}{2(\gamma - \kappa)\theta} \|\hat{z}^k - z^k\|^2 + \frac{\rho(2\rho\beta^2\theta^{-1} + \gamma\beta\theta)}{2(\gamma - \kappa)\theta^2} \{\|x^k - x^{k-1}\|^2 - \mathbb{E}_k[\|x^{k+1} - x^k\|^2]\} \\
&\quad + \frac{2\rho L_f^2}{(\gamma - \kappa)^2\theta^2} - \frac{\rho(\gamma\theta^2 - 2\theta(\rho + \kappa\beta) - 2\rho\beta^2\theta^{-1})}{2(\gamma - \kappa)\theta^2} \mathbb{E}_k[\|x^{k+1} - x^k\|^2] + \frac{\rho\mathbb{E}_k[\varepsilon_k]}{(\gamma - \kappa)\theta^2} \tag{54}
\end{aligned}$$

$$\begin{aligned}
&= \psi_{1/\rho}(z^k) + \frac{\rho\beta}{(\gamma - \kappa)\theta^2} \{\psi(x^k) - \mathbb{E}_k[\psi(x^{k+1})]\} \\
&\quad - \frac{\rho(\rho - \kappa\theta)}{2(\gamma - \kappa)\theta} \|\hat{z}^k - z^k\|^2 + \frac{\rho(2\rho\beta^2\theta^{-1} + \gamma\beta\theta)}{2(\gamma - \kappa)\theta^2} \{\|x^k - x^{k-1}\|^2 - \mathbb{E}_k[\|x^{k+1} - x^k\|^2]\} \\
&\quad + \frac{2\rho L_f^2}{(\gamma - \kappa)^2\theta^2} - \frac{\rho(\gamma\theta^2 - 2\theta(\rho + \kappa\beta) - 2\rho\beta^2\theta^{-1})}{2(\gamma - \kappa)\theta^2} \mathbb{E}_k[\|x^{k+1} - x^k\|^2] + \frac{\rho\mathbb{E}_k[\varepsilon_k]}{(\gamma - \kappa)\theta^2}, \tag{55}
\end{aligned}$$

where (54) uses the relation from (53). Last we re-arrangement the terms in (55) to get

$$\begin{aligned}
& \frac{\rho(\rho - \kappa\theta)}{2(\gamma - \kappa)\theta} \|\hat{z}^k - z^k\|^2 \\
&\leq \psi_{1/\rho}(z^k) - \mathbb{E}_k[\psi_{1/\rho}(z^{k+1})] + \frac{\rho\beta}{(\gamma - \kappa)\theta^2} \{\psi(x^k) - \mathbb{E}_k[\psi(x^{k+1})]\} \\
&\quad + \frac{\rho(2\rho\beta^2\theta^{-1} + \gamma\beta\theta)}{2(\gamma - \kappa)\theta^2} \{\|x^k - x^{k-1}\|^2 - \mathbb{E}_k[\|x^{k+1} - x^k\|^2]\} \\
&\quad + \frac{2\rho L_f^2}{(\gamma - \kappa)^2\theta^2} - \frac{\rho(\gamma\theta^2 - 2\theta(\rho + \kappa\beta) - 2\rho\beta^2\theta^{-1})}{2(\gamma - \kappa)\theta^2} \mathbb{E}_k[\|x^{k+1} - x^k\|^2] + \frac{\rho\mathbb{E}_k[\varepsilon_k]}{(\gamma - \kappa)\theta^2}.
\end{aligned}$$

Recalling that  $\|\nabla\psi_{1/\rho}(\hat{z}^k)\|^2 = \rho^2\|\hat{z}^k - z^k\|^2$ , we complete the proof.

### C.3 Proof of Lemma 3

By Lemma 2 we have that

$$\begin{aligned}
& \frac{\rho - \kappa\theta}{2\rho(\gamma - \kappa)\theta} \|\hat{z}^k - z^k\|^2 \\
&\leq \psi_{1/\rho}(z^k) - \mathbb{E}_k[\psi_{1/\rho}(z^{k+1})] + \frac{\rho\beta}{(\gamma - \kappa)\theta^2} \{\psi(x^k) - \mathbb{E}_k[\psi(x^{k+1})]\} \\
&\quad + \frac{\rho(2\rho\beta^2\theta^{-1} + \gamma\beta\theta)}{2(\gamma - \kappa)\theta^2} \{\|x^k - x^{k-1}\|^2 - \mathbb{E}_k[\|x^{k+1} - x^k\|^2]\} \\
&\quad + \frac{2\rho L_f^2}{(\gamma - \kappa)^2\theta^2} - \frac{\rho(\gamma\theta^2 - 2\theta(\rho + \kappa\beta) - 2\rho\beta^2\theta^{-1})}{2(\gamma - \kappa)\theta^2} \mathbb{E}_k[\|x^{k+1} - x^k\|^2] + \frac{\rho\mathbb{E}_k[\varepsilon_k]}{(\gamma - \kappa)\theta^2}. \tag{56}
\end{aligned}$$

Summing up the inequality (56) from  $k = 1$  to  $K$ , multiplying both sides by  $\gamma + \kappa > 0$  and taking expectation, we have

$$\begin{aligned}
& \frac{\rho - \kappa\theta}{2\rho\theta} \mathbb{E}[\|\nabla\psi_{1/\rho}(z^{k*})\|^2] \\
& \leq \frac{\gamma - \kappa}{K} \{\psi_{1/\rho}(z^1) - \mathbb{E}_k[\psi_{1/\rho}(z^{K+1})]\} + \frac{\rho\beta}{\theta^2 K} \{\psi(x^k) - \mathbb{E}_k[\psi(x^{k+1})]\} \\
& \quad + \frac{\rho(2\rho\beta^2\theta^{-1} + \gamma\beta\theta)}{2\theta^2 K} \|x^1 - x^0\|^2 + \frac{2\rho L_f^2 K}{(\gamma - \kappa)\theta^2} + \frac{\rho}{\theta^2 K} \sum_{k=1}^K \mathbb{E}_k[\varepsilon_k] \\
& \quad - \frac{\rho(\gamma\theta^2 - 2\theta(\rho + \kappa\beta) - 2\rho\beta^2\theta^{-1})}{2\theta^2 K} \sum_{k=1}^K \mathbb{E}[\|x^{k+1} - x^k\|^2] \\
& \leq \frac{(\gamma - \kappa + \rho\beta\theta^{-2})D}{K} + \frac{2\rho L_f^2}{(\gamma - \kappa)\theta^2} + \frac{\rho}{\theta^2 K} \sum_{k=1}^K \mathbb{E}_k[\varepsilon_k] \\
& \quad - \frac{\rho(\gamma\theta^2 - 2\theta(\rho + \kappa\beta) - 2\rho\beta^2\theta^{-1})}{2\theta^2 K} \sum_{k=1}^K \mathbb{E}[\|x^{k+1} - x^k\|^2] \tag{57}
\end{aligned}$$

where the last inequality uses  $x^0 = x^1$  and  $D = \max\{\psi_{1/\rho}(z^1) - \psi_{1/\rho}(z^*), \psi(x^1) - \psi(x^*)\}$ . Now we divide both sides of the inequality by  $\frac{\rho - \kappa\theta}{2\rho\theta}$  to get

$$\mathbb{E}[\|\nabla\psi_{1/\rho}(z^{k*})\|^2] \leq \frac{2\rho\theta}{\rho - \kappa\theta} \left[ \frac{(\gamma - \kappa + \rho\beta\theta^{-2})D}{K} + \frac{2\rho L_f^2}{(\gamma - \kappa)\theta^2} + \frac{\rho}{\theta^2 K} \sum_{k=1}^K \mathbb{E}_k[\varepsilon_k] \right].$$

Last we bound  $\sum_{k=1}^K \mathbb{E}[\varepsilon_k]$ . First, we have the following relations

$$\sum_{k=1}^K \|x^{k+1} - x^{k-\tau_k}\|^2 \leq \tau^2 \sum_{k=1}^K \|x^k - x^{k-1}\|^2 \leq \tau^2 \sum_{k=1}^K \|x^{k+1} - x^k\|^2,$$

where the first inequality is by **C1** and the second inequality uses the fact that  $x^0 = x^1$ . Similarly

$$\begin{aligned}
\sum_{k=1}^K \|x^{k+1} - x^{k-\tau_k}\|^2 & \leq \sum_{k=1}^K 2[\|x^k - x^{k-\tau_k}\|^2 + \|x^{k+1} - x^k\|^2] \\
& \leq 2(\tau^2 + 1) \sum_{k=1}^K \|x^{k+1} - x^k\|^2,
\end{aligned}$$

where the first inequality uses  $\|a + b\|^2 \leq 2\|a\|^2 + 2\|b\|^2$  and the second inequality re-uses the bound of the first term. Plugging the above bounds back into  $\sum_{k=1}^K \mathbb{E}[\varepsilon_k]$ , we successively deduce that

$$\begin{aligned}
\sum_{k=1}^K \mathbb{E}[\varepsilon_k] & = \sum_{k=1}^K \frac{\lambda(1 - \theta)}{2} \|x^k - x^{k-\tau_k}\|^2 + \sum_{k=1}^K \left( \theta + \frac{1}{2} \right) \lambda \mathbb{E}[\|x^{k+1} - x^{k-\tau_k}\|^2] \\
& \leq \lambda[(1 - \theta)(\tau^2 + 1) + (\theta + 1/2)\tau^2] \sum_{k=1}^K \mathbb{E}[\|x^{k+1} - x^k\|^2] \\
& = \lambda(3\tau^2/2 + \beta) \sum_{k=1}^K \mathbb{E}[\|x^{k+1} - x^k\|^2],
\end{aligned}$$

which implies

$$\begin{aligned} & \mathbb{E}[\|\nabla\psi_{1/\rho}(z^{k*})\|^2] \\ & \leq \frac{2\rho\theta}{\rho - \kappa\theta} \left[ \frac{(\gamma - \kappa + \rho\beta\theta^{-2})D}{K} + \frac{2\rho L_f^2}{(\gamma - \kappa)\theta^2} + \frac{\rho\lambda(3\tau^2 + 2\beta)}{2\theta^2 K} \sum_{k=1}^K \mathbb{E}[\|x^{k+1} - x^k\|^2] \right], \end{aligned} \quad (58)$$

and this completes the proof.

## C.4 Proof of Theorem 2

By **Lemma 3**, it remains to bound the quantity  $\sum_{k=1}^K \mathbb{E}[\|x^{k+1} - x^k\|^2]$ . To this end we consider the relation in (57), where we have

$$\begin{aligned} & \frac{\rho(\gamma\theta^2 - 2\theta(\rho + \kappa\beta) - 2\rho\beta^2\theta^{-1} - 3\lambda\tau^2 - 2\lambda\beta)}{2\theta^2 K} \sum_{k=1}^K \mathbb{E}[\|x^{k+1} - x^k\|^2] \\ & \leq \frac{(\gamma - \kappa + \rho\beta\theta^{-2})D}{K} + \frac{2\rho L_f^2}{(\gamma - \kappa)\theta^2}. \end{aligned}$$

Since we choose  $\beta, \gamma$  such that  $\gamma\theta^2 - 2\theta(\rho + \kappa\beta) - 2\rho\beta^2\theta^{-1} - 3\lambda\tau^2 - 2\lambda\beta > 0$ , then

$$\frac{\rho\lambda(3\tau^2 + 2\beta)}{2\theta^2 K} \sum_{k=1}^K \mathbb{E}[\|x^{k+1} - x^k\|^2] \leq \frac{\lambda(3\tau^2 + 2\beta) \left\{ \frac{(\gamma - \kappa + \rho\beta\theta^{-2})D}{K} + \frac{2\rho L_f^2}{(\gamma - \kappa)\theta^2} \right\}}{\gamma\theta^2 - 2\theta(\rho + \kappa\beta) - 2\rho\beta^2\theta^{-1} - 3\lambda\tau^2 - 2\lambda\beta}.$$

Plugging the bound back, we have

$$\begin{aligned} & \mathbb{E}[\|\nabla\psi_{1/\rho}(z^{k*})\|^2] \\ & \leq \frac{2\rho\theta}{\rho - \kappa\theta} \left[ \frac{(\gamma - \kappa + \rho\beta\theta^{-2})D}{K} + \frac{2\rho L_f^2}{(\gamma - \kappa)\theta^2} + \frac{\lambda(3\tau^2 + 2\beta) \left\{ \frac{(\gamma - \kappa + \rho\beta\theta^{-2})D}{K} + \frac{2\rho L_f^2}{(\gamma - \kappa)\theta^2} \right\}}{\gamma\theta^2 - 2\theta(\rho + \kappa\beta) - 2\rho\beta^2\theta^{-1} - 3\lambda\tau^2 - 2\lambda\beta} \right]. \end{aligned}$$

This completes our proof.

## D Improved Analysis of DSGD

In this section, we present the convergence analysis of DSGD. The proof follows a standard inexact potential reduction scheme and is done in the Euclidean setup, where **Lemma 5** and **Lemma 6** hold for  $d = \frac{1}{2}\|\cdot\|^2$ . After bounding inexactness using **Lemma 6**, the convergence result follows immediately.

### D.1 Proof of Lemma 4

Since  $\rho \geq \lambda + \kappa$ , by three-point lemma we get the following two relations

$$\langle g^{k-\tau_k}, x^{k+1} \rangle + \omega(x^{k+1}) + \frac{\gamma/k}{2} \|x^{k+1} - x^k\|^2 \leq \langle g^{k-\tau_k}, \hat{x}^k \rangle + \omega(\hat{x}^k) + \frac{\gamma/k}{2} \|\hat{x}^k - x^k\|^2 - \frac{\gamma/k - \kappa}{2} \|\hat{x}^k - x^{k+1}\|^2 \quad (59)$$

$$f(\hat{x}^k) + \omega(\hat{x}^k) + \frac{\rho}{2} \|\hat{x}^k - x^k\|^2 \leq f(x^{k+1}) + \omega(x^{k+1}) + \frac{\rho}{2} \|x^{k+1} - x^k\|^2 \quad (60)$$

Summing up (59) and (60) and taking expectation, we have

$$\begin{aligned}
& \frac{\gamma_k - \rho}{2} \mathbb{E}_k[\|x^{k+1} - x^k\|^2] - \frac{\gamma_k - \rho}{2} \|\hat{x}^k - x^k\|^2 + \frac{\gamma_k - \kappa}{2} \mathbb{E}_k[\|\hat{x}^k - x^{k+1}\|^2] \\
& \leq f(x^{k-\tau_k}, \xi^{k-\tau_k}) + \langle g^{k-\tau_k}, \hat{x}^k - x^{k-\tau_k} \rangle - f(\hat{x}^k) \\
& \quad + \mathbb{E}_k[f(x^{k+1})] - f(x^{k-\tau_k}, \xi^{k-\tau_k}) - \mathbb{E}_k[\langle g^{k-\tau_k}, x^{k+1} - x^{k-\tau_k} \rangle] \\
& \leq \frac{\lambda}{2} \|\hat{x}^k - x^{k-\tau_k}\|^2 + 2L_f \|x^{k+1} - x^{k-\tau_k}\|
\end{aligned} \tag{61}$$

where (61) follows from  $\lambda$ -weak convexity and Lipschitz continuity of  $f(x, \xi)$ . Re-arranging the terms,

$$\begin{aligned}
& \frac{\gamma_k - \kappa}{2} \mathbb{E}_k[\|\hat{x}^k - x^{k+1}\|^2] \\
& \leq \frac{\gamma_k - \rho}{2} \|\hat{x}^k - x^k\|^2 + \frac{\lambda}{2} \|\hat{x}^k - x^{k-\tau_k}\|^2 + 2L \mathbb{E}_k[\|x^{k+1} - x^{k-\tau_k}\|] - \frac{\gamma_k - \rho}{2} \mathbb{E}_k[\|x^{k+1} - x^k\|^2] \\
& \leq \frac{\gamma_k - \rho}{2} \|\hat{x}^k - x^k\|^2 + \lambda \mathbb{E}_k[\|x^{k+1} - x^{k-\tau_k}\|^2] + \lambda \mathbb{E}_k[\|\hat{x}^k - x^{k+1}\|^2] + 2L_f \mathbb{E}_k[\|x^{k+1} - x^{k-\tau_k}\|]
\end{aligned} \tag{62}$$

where (62) follows by Cauchy's inequality  $\|a + b\|^2 \leq 2\|a\|^2 + 2\|b\|^2$ . Now we re-arrange the terms and divide both sides by  $(\gamma_k - 2\lambda - \kappa)$  to derive

$$\begin{aligned}
& \mathbb{E}_k[\|\hat{x}^k - x^{k+1}\|^2] \\
& \leq \frac{\gamma_k - \rho}{\gamma_k - 2\lambda - \kappa} \|\hat{x}^k - x^k\|^2 + \frac{2\lambda}{\gamma_k - 2\lambda - \kappa} \mathbb{E}_k[\|x^{k+1} - x^{k-\tau_k}\|^2] + \frac{4L_f}{\gamma_k - 2\lambda - \kappa} \mathbb{E}_k[\|x^{k+1} - x^{k-\tau_k}\|] \\
& = \|\hat{x}^k - x^k\|^2 - \frac{\rho - 2\lambda - \kappa}{\gamma_k - 2\lambda - \kappa} \|\hat{x}^k - x^k\|^2 + \frac{2\lambda}{\gamma_k - 2\lambda - \kappa} \mathbb{E}_k[\|x^{k+1} - x^{k-\tau_k}\|^2] + \frac{4L_f}{\gamma_k - 2\lambda - \kappa} \mathbb{E}_k[\|x^{k+1} - x^{k-\tau_k}\|].
\end{aligned} \tag{63}$$

Last, we measure the reduction in potential function  $\mathbb{E}_k[\psi_{1/\rho}(x^k)]$  and successively deduce that

$$\begin{aligned}
& \mathbb{E}_k[\psi_{1/\rho}(x^{k+1})] \\
& = \mathbb{E}_k[f(\hat{x}^{k+1}) + \omega(\hat{x}^{k+1}) + \frac{\rho}{2} \|\hat{x}^{k+1} - x^{k+1}\|^2] \\
& \leq \mathbb{E}_k[f(\hat{x}^k) + \omega(\hat{x}^k) + \frac{\rho}{2} \|\hat{x}^k - x^{k+1}\|^2] \\
& \leq \mathbb{E}_k[f(\hat{x}^k) + \omega(\hat{x}^k) + \frac{\rho}{2} \|\hat{x}^k - x^k\|^2] - \frac{\rho(\rho - 2\lambda)}{2(\gamma_k - 2\lambda - \kappa)} \|\hat{x}^k - x^k\|^2 \\
& \quad + \frac{\rho\lambda}{2(\gamma_k - 2\lambda - \kappa)} \mathbb{E}_k[\|x^{k+1} - x^{k-\tau_k}\|^2] + \frac{2\rho L_f}{\gamma_k - 2\lambda - \kappa} \mathbb{E}_k[\|x^{k+1} - x^{k-\tau_k}\|] \\
& = \psi_{1/\rho}(x^k) - \frac{\rho(\rho - 2\lambda - \kappa)}{2(\gamma_k - 2\lambda - \kappa)} \|\hat{x}^k - x^k\|^2 \\
& \quad + \frac{\rho\lambda}{\gamma_k - 2\lambda - \kappa} \mathbb{E}_k[\|x^{k+1} - x^{k-\tau_k}\|^2] + \frac{2\rho L_f}{\gamma_k - 2\lambda - \kappa} \mathbb{E}_k[\|x^{k+1} - x^{k-\tau_k}\|].
\end{aligned} \tag{64}$$

where (64) holds by plugging (63) in. A simple re-arrangement completes the proof.



## D.2 Proof of Theorem 3

By the descent property revealed in **Lemma 4**, we telescope over  $k = 1, \dots, K$  and

$$\begin{aligned}
& \frac{\rho(\rho - 2\lambda - \kappa)}{2} \mathbb{E}[\|\hat{x}^{k^*} - x^{k^*}\|^2] \\
&= \frac{\rho(\rho - 2\lambda - \kappa)}{2K} \sum_{k=1}^K \|\hat{x}^{k^*} - x^{k^*}\|^2 \\
&\leq \frac{\gamma - 2\lambda - \kappa}{K} \{\psi_{1/\rho}(x^1) - \mathbb{E}_k[\psi_{1/\rho}(x^{K+1})]\} + \frac{\rho}{K} \sum_{k=1}^K \mathbb{E}_k[\lambda \|x^{k+1} - x^{k-\tau_k}\|^2 + 2L_f \|x^{k+1} - x^{k-\tau_k}\|] \\
&\leq \frac{(\gamma - 2\lambda - \kappa)D}{K} + \frac{\rho}{K} \left\{ \sum_{k=1}^K \mathbb{E}_k[\lambda \|x^{k+1} - x^{k-\tau_k}\|^2 + 2L_f \|x^{k+1} - x^{k-\tau_k}\|] \right\},
\end{aligned}$$

where the second inequality is due to  $\psi(x^*) \leq \mathbb{E}_k[\psi_{1/\rho}(x^{K+1})]$ . Now it remains to bound the error from the stochastic delays. Similar to (32),

$$\sum_{k=1}^K \mathbb{E}_k[\|x^{k+1} - x^{k-\tau_k}\|^2] \leq 2K \left( \frac{L_f + L_\omega}{\gamma} \right)^2 (\tau_{\sigma^2} + 2\bar{\tau} + 1),$$

On the other hand, we bound the first-order term with

$$\begin{aligned}
\sum_{k=1}^K \mathbb{E}_k[\|x^{k+1} - x^{k-\tau_k}\|] &= \sum_{k=1}^K \sum_{j=0}^{\infty} p_j \mathbb{E}_k[\|x^{k+1} - x^{k-j}\|] \\
&\leq \sum_{k=1}^K \sum_{j=0}^{\infty} p_j \sum_{l=0}^j \mathbb{E}_k[\|x^{k-l+1} - x^{k-l}\|] \\
&\leq \sqrt{2} \left( \frac{L_f + L_\omega}{\gamma} \right) \sum_{k=1}^K \sum_{j=0}^{\infty} j p_j \\
&= \sqrt{2} K \left( \frac{L_f + L_\omega}{\gamma} \right) \bar{\tau}.
\end{aligned}$$

Plugging the bound back, we deduce that

$$\begin{aligned}
& \frac{\rho(\rho - 2\lambda - \kappa)}{2} \mathbb{E}[\|\hat{x}^{k^*} - x^{k^*}\|^2] \\
&\leq \frac{(\gamma - 2\lambda - \kappa)D}{K} + \frac{\rho}{K} \left\{ \sum_{k=1}^K \mathbb{E}_k[\lambda \|x^{k+1} - x^{k-\tau_k}\|^2 + 2L_f \|x^{k+1} - x^{k-\tau_k}\|] \right\} \\
&\leq \frac{(\gamma - 2\lambda - \kappa)D}{K} + \frac{2\sqrt{2}\rho L_f (L_f + L_\omega) \bar{\tau}}{\gamma} + \frac{2\rho(L_f + L_\omega)^2 (\tau_{\sigma^2} + 2\bar{\tau} + 1)}{\gamma^2} \\
&\leq \frac{D}{\sqrt{K}\alpha} + \frac{2\sqrt{2}\rho L_f (L_f + L_\omega) \bar{\tau} \alpha}{\sqrt{K}} + \frac{2\rho\lambda(L_f + L_\omega)^2 (\tau_{\sigma^2} + 2\bar{\tau} + 1) \alpha^2}{K},
\end{aligned} \tag{65}$$

where (65) is by  $\gamma = \sqrt{K}/\alpha + 2\lambda + \kappa$ . The proof is complete after dividing both sides by  $\rho(\rho - 2\lambda - \kappa)$  and using the fact that  $\frac{1}{2}\|\hat{x}^k - x^k\|^2 = \frac{1}{2\rho^2}\|\nabla\psi_{1/\rho}(x)\|^2$ .

### D.3 Proof of Theorem 4

Recall that in the proof of DSPL, we actually used **A4** and the properties from **Proposition 1** that are deduced from **A1**, **A2**, **A3** and **B1**. Indeed, it is straightforward to verify that  $f_z(x, \xi) = \langle \nabla f(z, \xi), x - z \rangle$  satisfies **Proposition 1** given **A1**, **A2**, **A3**.

## E Additional Experiments

In this section, we present the additional experiments on blind deconvolution problem to further illustrate the efficiency of DSPL. The blind deconvolution problem, unlike robust phase retrieval, aims to recover two signals from their convolution and its mathematical formulation is given by

$$\min_{x, y \in \mathbb{R}^n} \frac{1}{m} \sum_{i=1}^m |\langle u_i, x \rangle \langle v_i, y \rangle - b_i| + \mathbb{I}\{\|x\|, \|y\| \leq \Delta\},$$

where  $\mathbb{I}\{\cdot\}$  denotes the indicator function,  $\{b_i\}$  are the measurements,  $\{(u_i, v_i)\}$  are the measuring data and  $x, y$  are the optimization variables corresponding to the signals. Similar to phase retrieval, we first present the detailed setup and then inspect the performance of DSPL in both real and simulated asynchronous environments.

### E.1 Experiment Setup

**Data Generation.** We use synthetic data for blind deconvolution problems.

**Synthetic Data.** We take  $m = 300, n = 100$  in the experiments of simulated delay and  $m = 1500, n = 150$  in the asynchronous environment. The data is generated similar to phase retrieval, where, given some conditioning parameter  $\kappa \geq 1$ , we compute  $U = Q_1 D_2, V = Q_2 D_2, Q \in \mathbb{R}^{m \times n}, q_{ij} \sim \mathcal{N}(0, 1)$  and  $D = \text{diag}(d), d \in \mathbb{R}^n, d_i \in [1/\kappa, 1], \forall i$ . Then two true signals are generated like  $x^*$  in phase retrieval and we random corruption is applied.

- 1) **Dataset.** In the asynchronous environment, we set  $\kappa = 1, p_{\text{fail}} = 0$  and in the simulated environment, we set  $\kappa = 1$  and  $p_{\text{fail}} \in \{0.2, 0.3\}$ .
- 2) **Initial point and Radius.** We generate  $x', y' \sim \mathcal{N}(0, I_n)$  and start from  $x^0 = x^1 = \frac{x'}{\|x'\|}, y^0 = y^1 = \frac{y'}{\|y'\|}$ .  $\Delta = 1000\|(x^0, y^0)\|$ .
- 3) **Stepsize.** We tune the stepsize parameter setting  $\gamma = \sqrt{K/\alpha}$ , where  $\alpha \in \{0.1, 0.5, 1.0\}$  in the asynchronous environment,  $\alpha \in [10^{-2}, 10^1]$  for synthetic data in the simulated environment.

The rest of the experiment setup are consistent with in phase retrieval.

### E.2 Asynchronous Environment

The experiments for blind deconvolution again justifies the effect of DSPL in its convergence behavior and robustness to the stochastic delays. By retaining the smooth structure of the inner composite function, DSPL gives a more accurate approximation of the original objective function only at cost of transmitting one more scalar (i.e., the inner objective value). Hence DSPL serves as a competitive alternative to DSGD when the problem enjoys composite structure (2) in the distributed setting.

### E.3 Simulated Environment

In the simulated experiments for blind deconvolution, we can see similar robustness of DSPL against delay and stepsize selection, which confirms our previous observations.

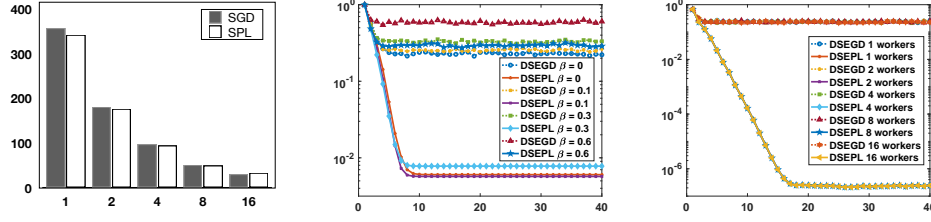


Figure 5: First: speedup in time and the number of workers. Second: progress of  $\|(x^k, y^k) - (x^*, y^*)\|$  in the first 40 epochs given 16 workers and  $\alpha = 0.5$ . Third: progress of  $f(x^k, y^k) - f(x^*, y^*)$  in the first 40 epochs given  $\beta = 0.1$  and different number of workers.

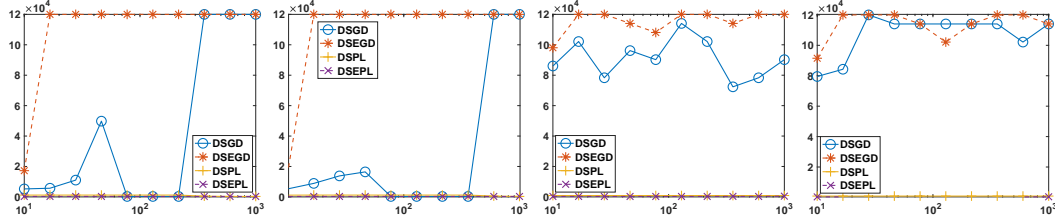


Figure 6: From left to right:  $(\kappa, p_{\text{fail}}) = (1, 0.2), \alpha = 4.6$ , Geometric and Poisson delays;  $(\kappa, p_{\text{fail}}) = (1, 0.3), \alpha = 2.1$ , Geometric and Poisson delays. The x-axis represents delay  $\tau$  and the y-axis gives the number of iterations to reach the stopping criterion.

## E.4 Proximal Sub-problems

This subsection shows how the sub-problems from DSPL and DSPL are solved for completeness. The results are a direct adaptation from [9] and interested readers can check [9] for the detailed derivations.

**Phase Retrieval Problem** In phase retrieval problem, we denote  $x$  to be the point where the stochastic model function is constructed and  $y$  to be the center of the proximal term. Then the DSPL proximal subproblem is given by

$$\min_x \left| \langle a, z \rangle^2 + 2\langle a, z \rangle \langle a, x - z \rangle - b \right| + \frac{\gamma}{2} \|x - y\|^2$$

and it admits closed-form solution when away from the boundary

$$x^+ = y + \text{Proj}_{[-1,1]} \left( -\frac{\delta}{\|\zeta\|^2} \right) \zeta,$$

where  $\delta = \gamma^{-1}(\langle a, z \rangle^2 + 2\langle a, z \rangle \langle a, x - z \rangle - b)$  and  $\zeta = 2\gamma^{-1}\langle a, z \rangle a$  and  $\text{Proj}_{[-1,1]}(\cdot)$  denotes projection onto the box  $[-1, 1]$ . When the algorithm hits the boundary of the indicator, we invoke a QCQP solver to compute the next iterate.

**Blind Deconvolution Problem** In the blind deconvolution problem, we use  $z = (z_x, z_y)$  to denote the point of model construction and  $w = (w_x, w_y)$  to denote the proximal center. Then the subproblem is given by

$$\min_{\|x\|, \|y\| \leq M} \left| \langle u, z_x \rangle \langle v, z_y \rangle + \langle v, z_y \rangle \langle u, x - z_x \rangle + \langle u, z_x \rangle \langle v, y - z_y \rangle - b \right| + \frac{\gamma}{2} [\|x - w_x\|^2 + \|y - w_y\|^2].$$

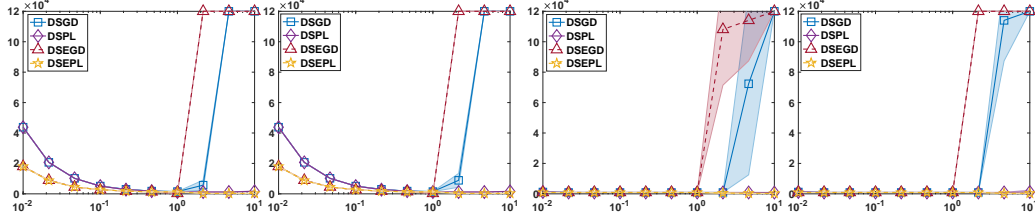


Figure 7: From left to right:  $(\kappa, p_{\text{fail}}) = (1, 0.2)$ , Geometric and Poisson delays with  $\tau = 10$ ;  $(\kappa, p_{\text{fail}}) = (1, 0.3)$ , Geometric and Poisson delays with  $\tau = 216$ .

First we assume that the constraints are inactive, then the solution is available in closed form

$$w^+ = w + \text{Proj}_{[-1,1]} \left( -\frac{\delta}{\|\zeta\|^2} \right) \zeta,$$

where

$$\begin{aligned} \delta &= \gamma^{-1} [\langle u, z_x \rangle \langle v, z_y \rangle + \langle v, z_y \rangle \langle u, w_x - z_x \rangle + \langle u, z_x \rangle \langle v, w_y - z_y \rangle - b] \\ \zeta &= \gamma^{-1} (\langle v, z_y \rangle u, \langle u, z_x \rangle v). \end{aligned}$$

Similarly, if either  $w_x^+$  or  $w_y^+$  goes beyond the domain, we apply QCQP solver to obtain the next iterate.